

# 1 CropSuite v1.0 - A comprehensive open-source crop 2 suitability model considering climate variability for 3 climate impact assessment

4 F. Zabel<sup>1</sup>, M. Knüttel<sup>1</sup>, B. Poschlod<sup>2</sup>

5 <sup>1</sup>Department of Environmental Sciences, University of Basel, 4056 Basel, Switzerland

6 <sup>2</sup>Center for Earth System Research and Sustainability, Universität Hamburg, 20144 Hamburg, Germany

7

8 *Correspondence to:* florian.zabel@unibas.ch

9

## 10 **Abstract.**

11 Increasing demand for agricultural land resources and changing climate conditions require for strategic land-use planning  
12 and the development of adaptation strategies. Therefore, information about the suitability of agricultural land is a  
13 prerequisite. Current suitability approaches often focus on single crops, can only be applied regionally and usually neglect  
14 the impact of climate variability on crop suitability. Here, we introduce CropSuite, a new comprehensive and easy-to-use  
15 crop suitability model that allows to overcome these shortcomings. It provides a graphical user interface (GUI) and a  
16 wide range of pre- and postprocessing options, including a tool for data analysis, which allows users to easily apply the  
17 model and analyze the results. Further, it includes a spatial downscaling approach for climate data, which enables crop  
18 suitability analysis at very high spatial resolution. CropSuite uses a fuzzy logic approach and is based on the assumption  
19 of Liebig's law of the minimum. An expandable number of environmental and socio-economic factors that impact on  
20 crop suitability can flexibly be integrated into CropSuite by determining membership functions. CropSuite allows for the  
21 consideration of irrigated and rainfed agricultural systems, vernalization requirements for winter crops, lethal temperature  
22 thresholds, photoperiodic sensitivity and several other limitations for crop growth. The model endogenously calculates  
23 and outputs climate-, soil-, and crop suitability, the optimal sowing- and harvest dates, the potential for multiple cropping,  
24 the (most) limiting factor(s), as well as the recurrence rate of potential crop failures according to the inter-annual climate  
25 variability.

26 In this study, we apply CropSuite for 48 crops at a spatial resolution of 30 arc seconds (1 km at the equator) for Africa.  
27 Thereby, we consider regionally important staple and cash crops that are usually understudied, such as coffee, cassava,  
28 banana, oil palm, cocoa, cowpea, groundnuts, mango, millet, papaya, rubber, sesame, sorghum, sugar cane, tobacco, and  
29 yams. We find that the consideration of climate variability for calculating crop suitability makes a significant difference  
30 on suitable areas, but also affects optimal sowing dates, and multiple cropping potentials. The most vulnerable regions

31 for climate variability are identified in Somalia, Kenya, Ethiopia, South Africa, and the Maghreb countries. The results  
32 provide valuable crop-specific information that can be further used for climate impact assessments, adaptation and land-  
33 use planning at global, regional, or local scale. CropSuite is provided open source and could be of interest for model  
34 developers, scientists, and a wide range of potential users and stakeholders, such as farmers, companies, GOs, and NGOs.

35

36 **Key Words: Agriculture, Africa, Optimal Sowing Dates, Multiple Cropping, Maize**

## 37 **1 Introduction**

38 Climate change poses major challenges for agricultural production and food security. With warming climate, agricultural  
39 suitability changes and suitable areas shift towards higher latitudes (Franke et al., 2021; Zabel et al., 2014). Crop  
40 suitability models allow for a quantitative evaluation of land for crop cultivation and can therefore assess how the  
41 suitability of land changes with changing climate. Contrary to mechanistic crop models (Jägermeyr et al., 2021;  
42 Jägermeyr et al., 2020; Müller et al., 2024), crop suitability models are based on empirical approaches but are less  
43 computational intensive and thus allow for the consideration of more crops at higher spatial resolution (Zabel et al., 2014).  
44 As a result, crop suitability models provide important insights for sustainable land-use planning and climate change  
45 adaptation, e.g. through cultivar change or land-use change. Akpoti et al. (2019) give an overview of existing crop  
46 suitability approaches. Most studies are applied at regional scale (Maleki et al., 2017; Bonfante et al., 2015; Ranjitkar et  
47 al., 2016), while just a few global approaches exist (Akpoti et al., 2019). In addition, most studies focus just on single  
48 crops and do not cover a variety of different crops (Ramirez-Villegas et al., 2013; Akpoti et al., 2020). Particularly for  
49 Africa, domestically consumed staple crops, such as yams and cassava are often overseen in current studies, due to minor  
50 economic relevance, despite their regional importance for food security (Chapman et al., 2020; Chemura et al., 2024;  
51 Van Zonneveld et al., 2023; Karl et al., 2024). So far, none of the existing approaches systematically considers the impact  
52 of climate variability on crop suitability, which is a major shortcoming, since climate variability is expected to increase  
53 with climate warming and has a strong impact on agriculture (Vogel et al., 2019; Goulart et al., 2021; Ipcc, 2021).

54 The aim of this study is to introduce the CropSuite model, which is based on the crop suitability approach developed by  
55 Zabel et al. (2014) and has continuously been further developed by Cronin et al. (2020) and Schneider et al. (2022a). The  
56 model has previously been applied globally for 23 crops for different climate scenarios (Zabel, 2022). The model applies  
57 Liebig's law of the minimum, assuming that the scarcest resource limits the crop growth. CropSuite is based on a fuzzy  
58 logic approach where, in contrast to Boolean logic, the truth value of variables can be any real number between 0 and 1.  
59 In fuzzy logic, fuzzy sets consist of elements whose degrees of memberships are described by membership functions  
60 (Zadeh L.A., 1965). In our approach, we apply fuzzy logic to create crop-specific membership functions (Fig. 1)  
61 describing the abiotic crop requirements between 0 (not suitable) and 100 (highly suitable) according to various climatic,  
62 soil, and topographic variables (Zabel et al., 2014). This approach is adopted, fundamentally redesigned and expanded

63 with the goal to provide a comprehensive but easy-to-use and flexible open-source model that can be applied e.g. by  
 64 scientists, farmers, companies, national or international GOs, and NGOs. Therefore, CropSuite is now completely  
 65 reprogrammed in Python and consists of a graphical user interface (GUI), as well as several pre-processing and analysis  
 66 tools, e.g. for selecting a simulation domain, statistically downscaling the climate data, interpolating the membership  
 67 functions and automatically analyzing and mapping the results. In addition, CropSuite is complemented with a new  
 68 approach to consider the impact of climate variability on crop suitability. It includes a user manual, which is provided  
 69 together with the source code (Knüttel and Zabel, 2024).

## 70 2 Methods and Data

71 For this study, we apply CropSuite for Africa at 30 arc seconds spatial resolution (approximately 1 km<sup>2</sup> at the equator)  
 72 with the goal to simulate relevant but often overseen crops for this continent (Van Zonneveld et al., 2023). Table 1 shows  
 73 the 48 crops, that have been parameterized and simulated with CropSuite.

74  
 75 **Table 1: List of 48 considered crops simulated with CropSuite.** Binomial names are given in brackets.

1. Alfalfa ( <i>Medicago sativa</i> )	25. Olive ( <i>Olea europaea</i> )
2. Arabica Coffee ( <i>Coffea arabica</i> )	26. Onion ( <i>Allium cepa</i> )
3. Avocado ( <i>Persea americana</i> )	27. Papaya ( <i>Carica papaya</i> )
4. Banana ( <i>Musa spp.</i> )	28. Pea ( <i>Pisum sativum</i> )
5. Barley ( <i>Hordeum vulgare</i> )	29. Pineapple ( <i>Ananas comosus</i> )
6. Beans ( <i>Phaseolus vulgaris</i> )	30. Potato ( <i>Solanum tuberosum</i> )
7. Cabbage ( <i>Brassica oleracea</i> )	31. Rapeseed ( <i>Brassica napus</i> )
8. Carrot ( <i>Daucus carota</i> )	32. Rice ( <i>Oryza sativa</i> )
9. Cashew ( <i>Anacardium occidentale</i> )	33. Robusta Coffee ( <i>Coffea canephora</i> )
10. Cassava ( <i>Manihot esculenta</i> )	34. Rubber ( <i>Hevea brasiliensis</i> )
11. Castor Bean ( <i>Ricinus communis</i> )	35. Rye ( <i>Secale cereale</i> )
12. Chickpea ( <i>Cicer arietinum</i> )	36. Safflower ( <i>Carthamus tinctorius</i> )
13. Citrus ( <i>Citrus spp.</i> )	37. Sesame ( <i>Sesamum indicum</i> )
14. Cocoa ( <i>Theobroma cacao</i> )	38. Sorghum ( <i>Sorghum bicolor</i> )
15. Coconut ( <i>Cocos nucifera</i> )	39. Soy ( <i>Glycine maximum</i> )
16. Cotton ( <i>Gossypium hirsutum</i> )	40. Sugar Cane ( <i>Saccharum officinarum</i> )
17. Cowpea ( <i>Vigna unguiculata</i> )	41. Sunflower ( <i>Helianthus annuus</i> )
18. Green Pepper ( <i>Capsium annuum</i> )	42. Sweet Potato ( <i>Ipomoea batatas</i> )
19. Groundnut ( <i>Arachis hypogaea</i> )	43. Tea ( <i>Camellia sinensis</i> )
20. Guava ( <i>Psidium guajava</i> )	44. Tobacco ( <i>Nicotiana tabacum</i> )
21. Maize ( <i>Zea mays</i> )	45. Tomato ( <i>Solanum lycopersicum esculentum</i> )
22. Mango ( <i>Mangifera indica</i> )	46. Watermelon ( <i>Colocynthis citrullus</i> )
23. Millet ( <i>Pennisetum americanum</i> )	47. Wheat ( <i>Triticum aestivum</i> )
24. Oil Palm ( <i>Elaeis guineensis</i> )	48. Yams ( <i>Dioscorea</i> )

76

77 We simulate a 20-year time period from 1991 to 2010 using the Climate Hazards group Infrared Precipitation with  
78 Stations (CHIRPS) v2.0 daily data for precipitation (Funk et al., 2015) and the Climate Hazards Center Infrared  
79 Temperature with Stations (CHIRTS) v1.0 data for temperature (Funk et al., 2019; Verdin et al., 2020) at 2.5 arc minutes  
80 spatial resolution for Africa. Both data sets provide climatologies at daily to monthly resolution based on a combination  
81 of satellite remote sensing and climate stations. They benefit from long-term geostationary satellite observations,  
82 delivering consistent data since the 1980s at the quasi-global (50°S-50°N) scale.

83 In addition, soil and terrain information is required. Table 2 gives an overview of the soil and terrain data used for this  
84 study. Soil data is mainly based on ISRIC SoilGrids (Hengl et al., 2017), which has a spatial resolution of 250 m but is  
85 also provided at 1000 m spatial resolution. This data is reprojected to WGS84 and spatially interpolated using nearest  
86 neighbor to the spatial resolution of 30 arc seconds applied in this study. Base saturation, gypsum, and exchangeable  
87 sodium content (ESP, sodicity) are taken from the WISE database at a spatial resolution of 30 arc seconds (Batjes, 2016).  
88 For electric conductivity, the ISRIC Global Soil Salinity Map with a resolution of 250 m is used (Ivushkin et al., 2019).  
89 In contrast to the harmonized world soil database (HWSD) (Fao et al., 2012), the ISRIC soil datasets do not contain a  
90 layer for texture class. For this reason, the texture class is determined using the sand and clay layer of SoilGrids according  
91 to the United States Department of Agriculture (USDA) triangular diagram of soil texture classes (Fao et al., 2012). For  
92 soil depths greater than 200 cm up to 50 m, the ISRIC dataset on absolute depth to bedrock (Hengl et al., 2017) is  
93 complemented with the dataset from Pelletier et al. (2016), which covers soil depths up to 200 cm.

94 Available soil layers can be weighted in CropSuite as required. The SoilGrids datasets provide information for six depths:  
95 0-5 cm, 5-15 cm, 15-30 cm, 30-60 cm, 60-100 cm, and 100-200 cm (Hengl et al., 2017; Hengl et al., 2014). According  
96 to Sys et al. (1991), soil properties have different effects on crop suitability depending on the soil layer. Accordingly, we  
97 use weighting factors as proposed by Sys et al. (1991) (see Table 2). The different distribution of the soil depths between  
98 the SoilGrids data and the weighting factors by Sys et al. (1991) is taken into account by using a proportional weighting  
99 of the SoilGrids layers. Terrain data are taken from the Shuttle Radar Topography Mission (SRTM) data set (Farr et al.,  
100 2007), which are used to calculate the slope at the applied spatial resolution. Please be aware that a coarser spatial  
101 resolution generally reduces the slope, which could result in an underestimation of possible slope limitations in  
102 mountainous regions. A possible terracing could remove the restriction due to the slope but usually terraces are too small  
103 to be considered at the aggregated spatial resolution of 30 arc seconds of the SRTM data in this study.

104

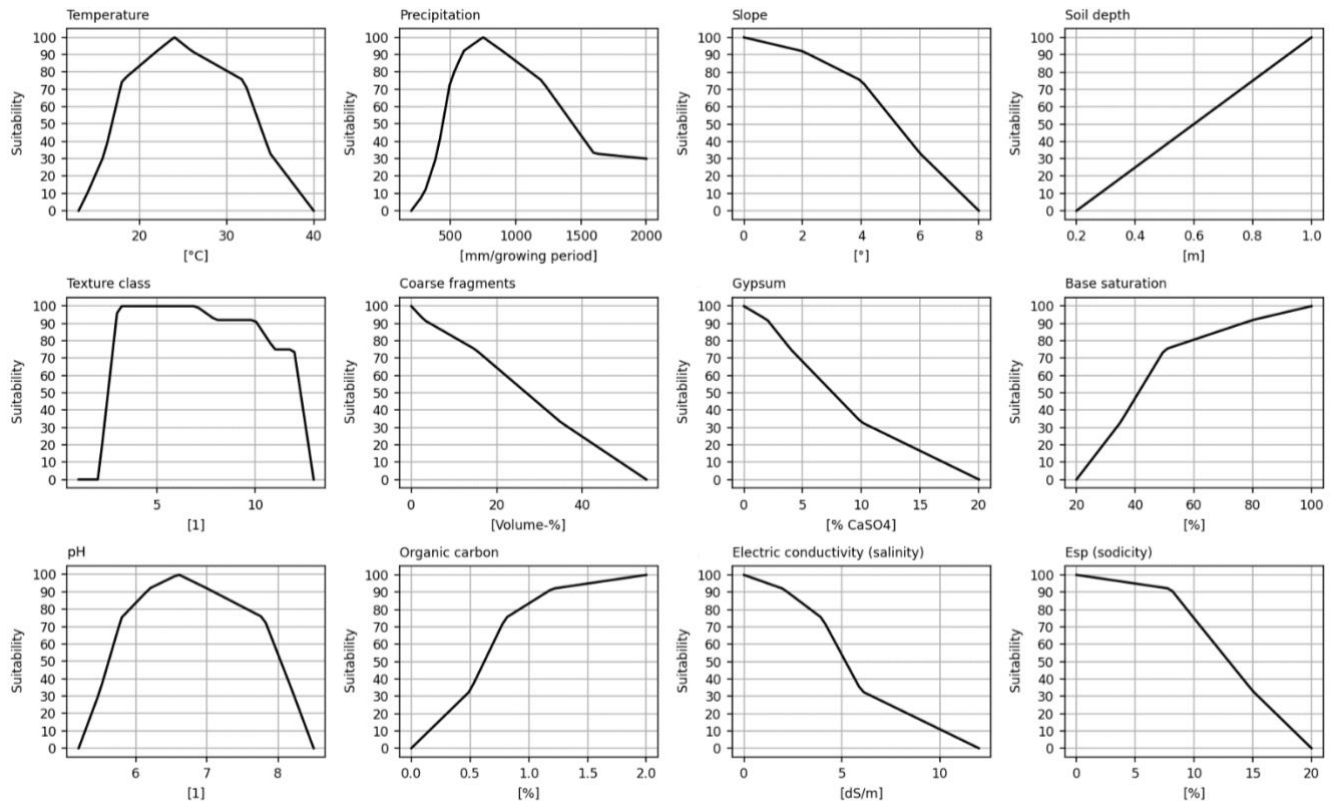
105 **Table 2: Soil and terrain data used in this study and the applied weighting of the different soil layers.**

<b>Parameter</b>	<b>Source</b>	<b>Weighting</b>
Base Saturation	ISRIC Harmonized Dataset of Derived Soil Properties for the World (WISE30sec) (Batjes, 2016)	Only Top Soil
Coarse Fragments	ISRIC SoilGrids 250m (Hengl et al., 2017)	0 - 25 cm: 2.0 25 - 50 cm: 1.5 50 - 75 cm: 1.0

		75 - 100 cm: 0.75 100 - 125 cm: 0.5 125 - 150 cm: 0.25
Electric Conductivity	ISRIC Global Soil Salinity Map (Ivushkin et al., 2019)	Only Top Soil
Gypsum Content	ISRIC Harmonized Dataset of Derived Soil Properties for the World (WISE30sec) (Batjes, 2016)	Only Top Soil
Organic Carbon Content	ISRIC SoilGrids 250m (Hengl et al., 2017)	0 - 25 cm: 2.0 25 - 50 cm: 1.5 50 - 75 cm: 1.0 75 - 100 cm: 0.75 100 - 125 cm: 0.5 125 - 150 cm: 0.25
Soil pH	ISRIC SoilGrids 250m (Hengl et al., 2017)	0 - 5 cm: 0.33 5 - 15 cm: 0.33 15 - 30 cm: 0.33
Sodicity	ISRIC Harmonized Dataset of Derived Soil Properties for the World (WISE30sec) (Batjes, 2016)	Only Top Soil
Soil Depth	ISRIC SoilGrids 2017 (Soil Depth <= 200 cm) (Hengl et al., 2017)  Pelletier et al. (2016) (Soil Depth > 200 cm)	No Weighting
Texture Class	Texture class calculated from ISRIC SoilGrids 250m clay and sand content (Hengl et al., 2017) according to USDA (Fao et al., 2012)	0 - 25 cm: 2.0 25 - 50 cm: 1.5 50 - 75 cm: 1.0 75 - 100 cm: 0.75 100 - 125 cm: 0.5 125 - 150 cm: 0.25
Slope	SRTM aggregated to 30 arcsec (Farr et al., 2007)	No Weighting

106  
107 Membership functions for temperature, precipitation, slope, soil depth, texture class, coarse fragments, gypsum, base  
108 saturation, pH, organic carbon, electric conductivity, sodicity (Fig. 1) are defined for the considered 48 crops relying on  
109 information from Sys et al. (1993), which provide membership functions for most of the considered crops. Additionally,  
110 data from the EcoCrop database, which provides crop ecological requirements for more than 2500 plant species (Fao,  
111 2024), is used for Cowpea, Rye, and Yams. CropSuite in principle allows the flexible addition of any further membership  
112 function and dataset that is relevant for the use case.

113 Nutrient deficits, such as nitrogen content are not considered in our approach, since according to our definition of crop  
114 suitability, they are not a decisive factor for the suitability of crops but rather depend on the crop management.  
115 Accordingly, we do not consider any soil tillage that can affect the soil properties, such as liming, which can influence  
116 the pH value.



117

118 **Figure 1: Membership functions exemplarily for maize** with a growing cycle of 110 days for considered climatic (mean temperature  
 119 over the growing cycle, total precipitation over the growing cycle), topographic (slope), and soil constraints (soil depth, texture class,  
 120 coarse fragments, gypsum, base saturation, pH, organic carbon, salinity, sodicity).

121 Sys et al. (1993) uses a classification system with 6 classes, ranging from N2 as unsuitable to S0 as highly suitable. In  
 122 this study, we dismiss the N1 class due to a vague definition and differentiate three suitability classes, marginally,  
 123 moderately, and highly suitable (Table 3).

124

125 **Table 3: Crop suitability classification system as used in this study compared to Sys et al. (1993).**

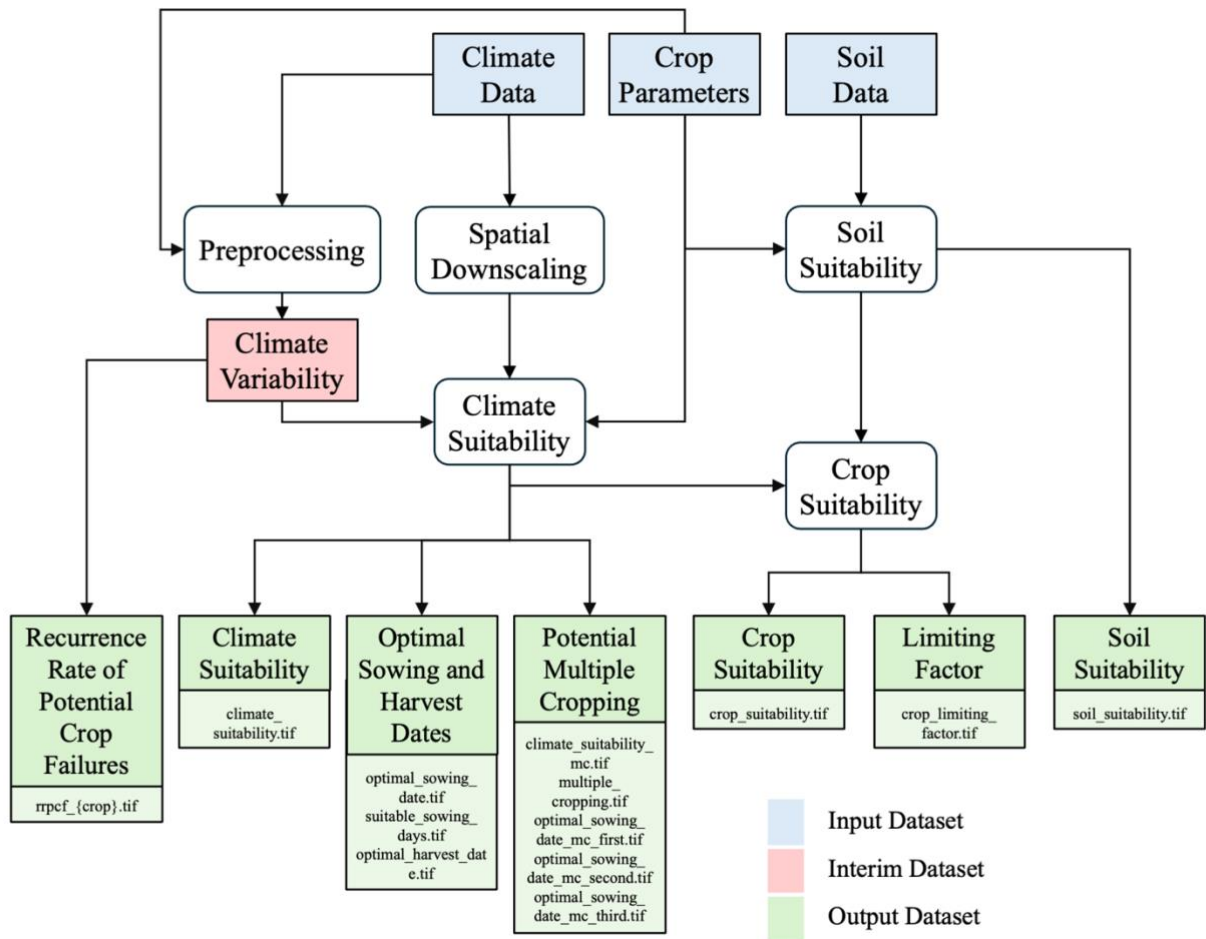
Suitability classes according to Sys et al.	Suitability range	Suitability classes used in this study
S0 (highly suitable)	100	75 – 100 (highly suitable)
S1 (very suitable)	80 – 99	
S2 (moderately suitable)	60 – 79	33 – 74 (moderately suitable)
S3 (marginally suitable)	40 – 59	1 – 32 (marginally suitable)
N1 (actually unsuitable and potentially suitable)	20 – 39	0 (unsuitable)
N2 (unsuitable)	0 - 19	

## 126 2.1 The CropSuite Model

127 Figure 2 shows the workflow and outputs of CropSuite, which first calculates a climate suitability (considering all climate  
 128 constraints) and then calculates a soil suitability (considering all soil and topography constraints). Both data records can

129 be output separately. Thereby, CropSuite applies Liebig's law of the minimum, for both the climate and the soil suitability  
130 by choosing the lowest suitability value between the different soil parameters and climate variables respectively. Finally,  
131 the crop suitability is calculated from the combination of both climate and soil suitability by again following Liebig's  
132 law of the minimum, which means that the lowest suitability value between climate and soil suitability is chosen, since  
133 it restricts overall crop suitability. The most limiting factor is identified as the parameter that imposes the greatest  
134 constraint on growth for a specific crop. In addition, the magnitude of the constraint is output for each input factor.  
135 Overall, CropSuite allows for a variety of outputs on optimal sowing- and harvest dates, suitable sowing days, multiple  
136 cropping potentials, the limiting factor, and the recurrence rate of potential crop failures. Output data format can be set  
137 to GeoTIFF or NetCDF.

138 CropSuite includes a pre-processing procedure which creates intermediate results for climate variability. Since climate  
139 model data are usually available at relatively coarse spatial resolution, CropSuite has implemented a spatial downscaling  
140 module for the climate data, which allows the model to be applied at very high spatial resolution from global to regional  
141 to local scale. In this study, we apply a statistical downscaling to the climate data, refining the spatial resolution from 2.5  
142 arc minutes to 30 arc seconds. In principle, the targeted spatial resolution can be set in CropSuite but is limited to the  
143 available resolution of the additional input data, such as the soil data, whereas for the climate data, two different statistical  
144 spatial downscaling methods are implemented requiring little computational effort. The first methodology is based on an  
145 altitude regression for temperature (Marke et al., 2014), where the temperature gradients are extracted from the climate  
146 model data itself via a moving window that can be set in size. Thereby, the extracted gradients must remain within the  
147 natural boundaries for wet and dry adiabatic temperature gradients. The second downscaling methodology uses the  
148 historical high-resolution spatial patterns for monthly temperature and precipitation taken from WorldClim at 30 arc  
149 seconds spatial resolution (Fick and Hijmans, 2017). To downscale a coarse-resolution grid cell, all fine-resolution  
150 WorldClim grid cells within the coarse-resolution cell are selected and aggregated per month. On this basis, additive  
151 factors are calculated for temperature and multiplicative factors for precipitation separately for each month. Thereby the  
152 sum (mean) of these additive (multiplicative) factors within the coarse-resolution cell amounts 0 (1). Considering the  
153 monthly seasonality, these factors are applied to the coarse-resolution climate data, imprinting the spatial pattern of the  
154 high-resolution reference data onto the coarse climate data at daily time step. Both downscaling methods conserve mass  
155 and energy from the climate input data by iteratively minimizing residuals over the simulation domain. For a more  
156 advanced statistical downscaling to kilometer-scale, the expert user may apply more complex topographical downscaling  
157 methods (Daly et al., 1994; Fiddes et al., 2022; Karger et al., 2023) or downscaling based on machine learning (Damiani  
158 et al., 2024; Wang et al., 2021) outside of CropSuite. Furthermore, we do not recommend applying the implemented  
159 downscaling methods with high scaling factors from very coarse (hundreds of kilometers) to very high (single kilometer)  
160 resolution.



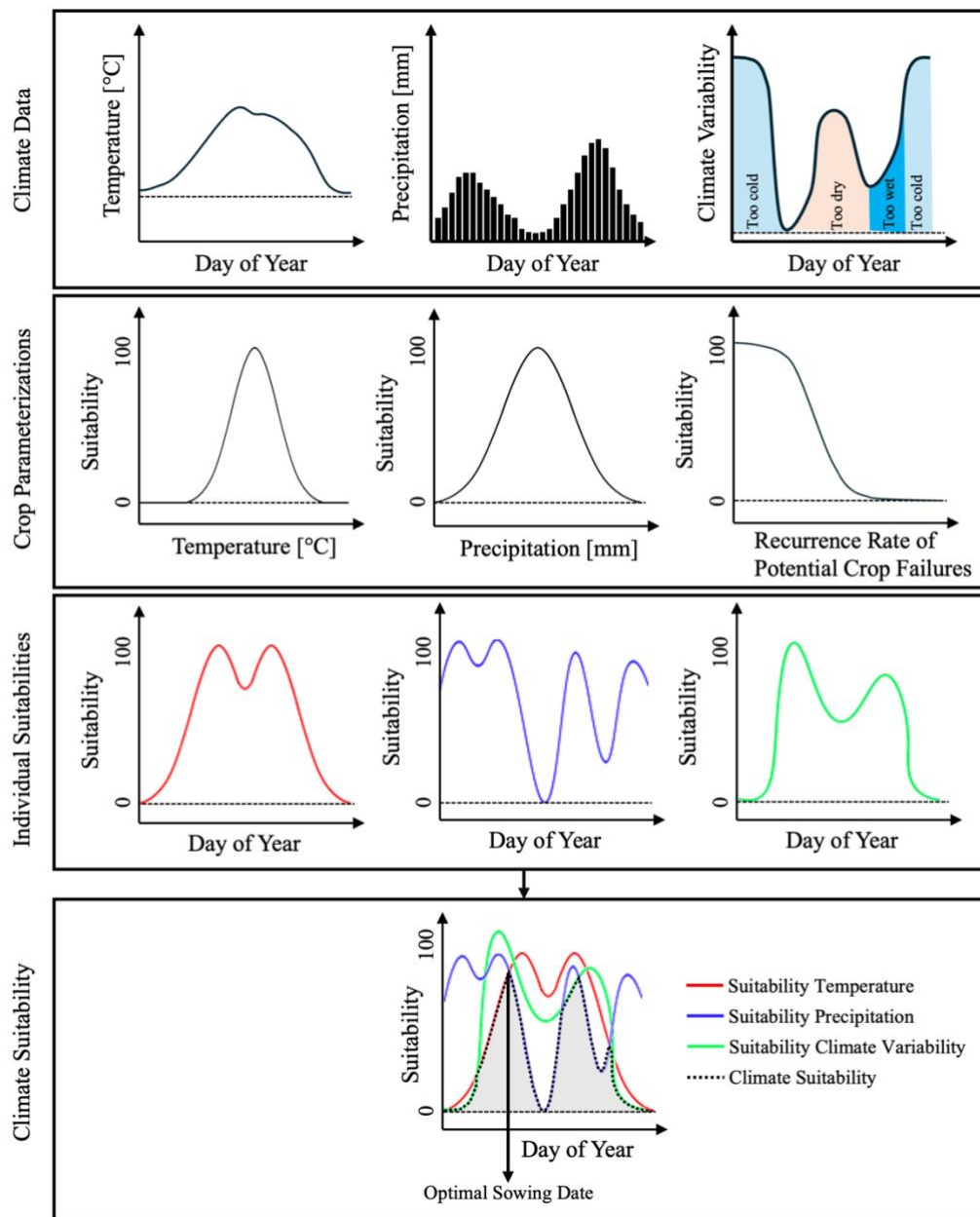
161

162 **Figure 2: CropSuite workflow.** Input data in blue, intermediate results in red and output data in green. The processing steps are  
 163 shown in white.

164 CropSuite requires daily climate data as an input for temperature and precipitation. As climate models tend to produce  
 165 too many days with low-intensity precipitation called “drizzle bias” (Chen et al., 2021), days with aggregated daily  
 166 precipitation values below 1 mm per day are considered to be dry days (Sun et al., 2006). This threshold can be set in the  
 167 model. Both downscaled temperature and precipitation data and the calculated datasets for climate variability are used to  
 168 calculate the climate suitability. Therefore, the crop-specific membership functions determine the suitability according  
 169 to the average temperature, total precipitation and the recurrence rate of potential crop failures over the length of the  
 170 growing cycle (time from sowing till maturity) for each day of year (DOY). Thereby, the suitability value for each DOY  
 171 refers to the average conditions during the growing cycle from that DOY, which corresponds to the sowing date, until  
 172 maturity, determined by the length of the growing cycle which is set in the crop parameterization for each crop. For  
 173 perennial crops, the length of the growing cycle is set to 365 days. Climate suitability throughout the year is then identified



174 by selecting the minimum value (most limiting) of the three individual suitabilities for temperature, precipitation, and  
 175 climate variability. As shown in Fig. 3, the DOY with the highest climate suitability value over the year finally determines  
 176 the optimal sowing date for annual crops (optimal planting date for rice, which is not sown, but planted as a seedling in  
 177 wet rice cultivation). For perennial crops this is set to 1.



178  
 179 **Figure 3: Schematic illustration of the determination of climate suitability, the optimal sowing date and the limiting factor.** The  
 180 input data shows the annual course of temperature, precipitation and the recurrence rate of potential crop failure, indicating whether it  
 181 is too cold, too dry, or too wet. The crop parameterizations show the membership functions resulting in the individual suitability values

182 for each DOY for either temperature (red line), precipitation (blue line), and climate variability (green line). Climate suitability  
183 throughout the year (black dashed line) results from the lowest of the three curves (most limiting) on any day. The highest value of  
184 climate suitability over the year finally determines the optimal sowing date. The limiting factor is the most constraining factor at this  
185 point.

186 For annual crops, CropSuite also calculates the potential for multiple harvests without considering crop rotation. Between  
187 harvest and reseeded, we assume a certain time period (21 days in this study) for field work and processing, which can  
188 be set flexibly in the model. Accordingly, all possible combinations of sowing dates are tested with the aim to maximize  
189 climatic suitability to achieve the highest sum of climatic suitability within a year. The optimal sowing dates are selected  
190 from the best sowing date combinations, resulting in one, two, or three sowing dates per year. A multiple cropping layer  
191 is output that shows how often a crop can be harvested.

192 CropSuite distinguishes between rainfed and irrigated agricultural systems, which can be selected before starting the  
193 simulation. For the irrigated case, precipitation is not considered as a constraining factor with consequences for all further  
194 calculations, affecting e.g. the climate variability, the optimal sowing date, and the multiple cropping. For this study, we  
195 separately simulated both, rainfed and irrigated options for all crops. In the post-processing, we combined both datasets  
196 according to the irrigated areas dataset by Meier et al. (2018) (Fig. S1), which is available at 30 arc-seconds spatial  
197 resolution.

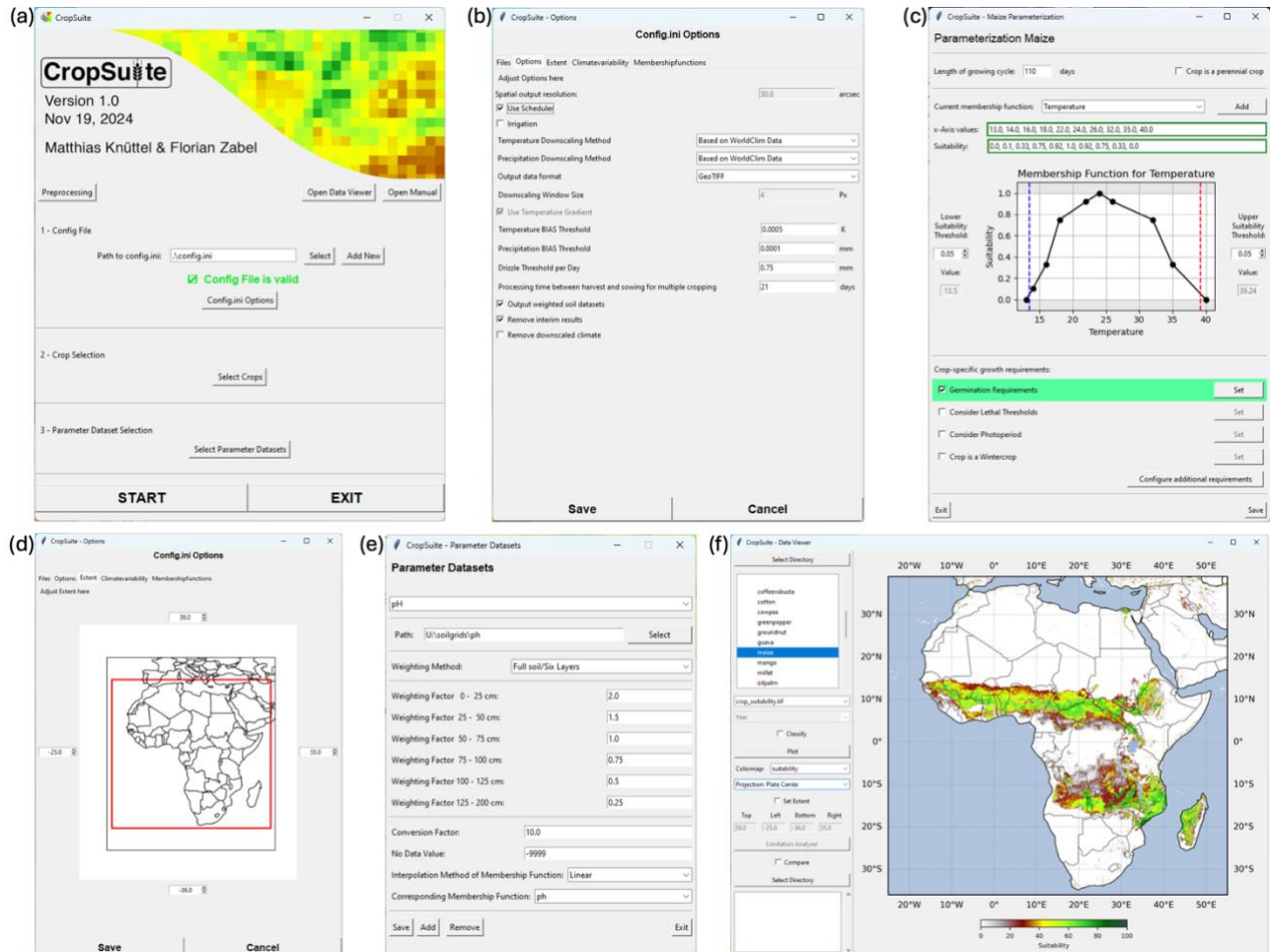
198 For germination, crop-specific temperature and soil water requirements can be set in the model. The latter can be  
199 considered for rainfed conditions by defining a certain amount of precipitation within a certain period of time after  
200 sowing.

201 Some crops, such as soybean have a high photoperiodic sensitivity which can limit their suitability (Cober and Morrison,  
202 2010; Abdulai et al., 2012). Therefore, crop-specific photoperiodic sensitivity can be considered in CropSuite by defining  
203 a maximum and minimum day length in average over the growing cycle.

204 Additional lethal climatic limitations can be taken into account in CropSuite. We assume permafrost on areas with an  
205 average annual temperature below 0° C, which is computed from the downscaled climate input data. A maximum lethal  
206 temperature threshold of >40°C in average over the growing cycle is set for all crops (Asseng et al., 2021). In addition, a  
207 minimum and maximum threshold for the lethal temperature over a certain consecutive number of days can be set in the  
208 model crop-specifically. Further, the maximum number of consecutive dry days can be set dependent on the  
209 crop. CropSuite allows for the consideration of vernalization requirements for winter crops. Therefore, crop-specific  
210 temperature requirements with minimal and maximal temperature thresholds for a certain number of vernalization  
211 effective days can be configured in the model. Accordingly, CropSuite simulates for each location, if and when these  
212 vernalization requirements are fulfilled, which impacts on the length of the vernalization period and the optimal sowing  
213 date. An offset of days from sowing to the start of the vernalization period can optionally be added.

214 A GUI is available for CropSuite that allows users to easily set-up the model, parameterize the crop requirements and the  
215 membership functions (Fig. 4a-e), and to start the simulations. Further, new membership functions can be created, an  
216 unlimited number of crop-specific requirements can be defined, and any additional data can be added, which can be

217 flexibly assigned to the defined membership functions (Fig. 4e). Moreover, new crops or crop varieties can be added.  
 218 The GUI also allows for the visualization, analysis and comparison of the results (Fig. 4f).



219  
 220 **Figure 4: Graphical User Interface of CropSuite.** (a) shows the main screen, (b) exemplarily shows available model settings, (c)  
 221 shows the available options for crop parameterizations exemplarily for maize, (d) shows the window to set-up the simulation domain,  
 222 (e) exemplarily shows the set-up of a parameter dataset for soil pH, and (f) shows the integrated data viewer in CropSuite.

## 223 2.2 Climate Variability

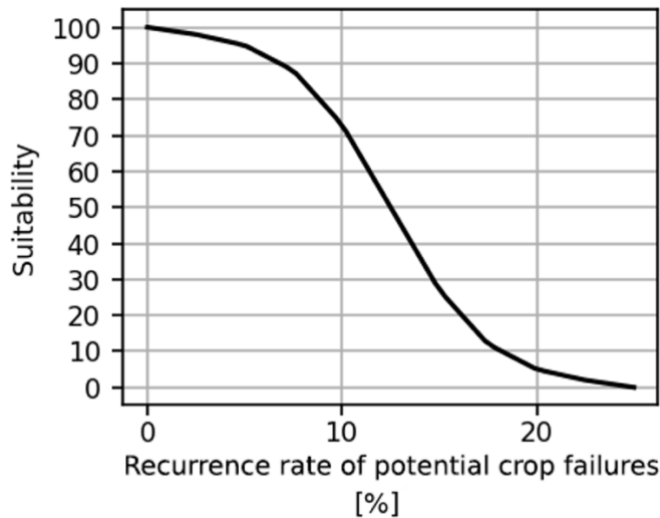
224 In addition to several improvements and redesigns, one of the most important advancements in CropSuite is the  
 225 consideration of climate variability for the assessment of crop suitability. Usually, crop suitability models consider long-  
 226 term climate averages, e.g. 10, 20 or 30-year periods and climatic trends that affect crop suitability (Ramirez-Villegas et  
 227 al., 2013; Schneider et al., 2022b). They are not designed so simulate seasonal yields, as for instants mechanistic crop  
 228 models do (Jägermeyr et al., 2021). However, existing crop suitability approaches may overestimate crop suitability when  
 229 only long-term averages are considered, because a high climatic variability may result in a high frequency of unsuitable

230 years, which would result in crop failures. This would however significantly increase the risk for farmers that require  
231 stable and plannable conditions. As a result, a farmer may conclude that the risk of crop failures due to unstable climate  
232 conditions in a certain region is too high for being suitable for crop cultivation. As such, climate variability is not a purely  
233 ecological limitation but depends on the socio-economic circumstances of how farmers deal with the risk of crop failure.  
234 We developed an approach that allows for the consideration of climate variability, and thus the implicit integration of  
235 socio-economic limitations in the suitability assessment of crops.

236 Therefore, we specify a crop-specific lower and upper threshold for temperature and precipitation. We recommend these  
237 thresholds between the higher and lower 5% and 10% suitability values of the crop-specific membership function,  
238 respectively (Figs. 1, 4c). If the suitability of the membership function does not approach 0 at its high (low) limit, we  
239 recommend setting the threshold to the highest (lowest) value of the membership function. This is the case for the wet  
240 limit of the precipitation membership function for maize (see Fig. 4c). For each year within a given period of time (here  
241 we use 20-year time periods), it is tested and totaled, how often these thresholds exceed or fall below during the growing  
242 cycle for all possible sowing dates (January 1<sup>st</sup> until December 31<sup>st</sup>). As a result, a variability dataset is generated for each  
243 DOY, indicating the number of years in which at least either the temperature or the precipitation exceeds or falls below  
244 the threshold values. The number of years is divided by the length of the time period (here 20 years) to obtain the  
245 recurrence rate of potential crop failures. This data can be stored as a two-dimensional raster file for perennial crops or  
246 as a three-dimensional raster file for non-perennial crops, with each of the 365 DOYs representing the condition for the  
247 respective sowing day.

248 For rainfed agricultural systems, cases that are considered for climate variability include excessively high or low  
249 temperatures and precipitation, while for irrigated agricultural systems, only excessively high or low temperatures and  
250 excessively high precipitation are considered, to address potential water logging, plant diseases or root rotting. Due to  
251 computational limitations, the preprocessing of the climate variability is carried out at the resolution of the input climate  
252 data (2.5 arc minutes) and is further interpolated bilinearly to the output resolution of 30 arc seconds.

253 Finally, we introduce a membership function defining the impact of climate variability on crop suitability. As shown in  
254 Fig. 5, a sigmoid is adopted for the course of the function. According to expert knowledge, we set this sigmoid function  
255 in a way that it reduces suitability to 0 when the recurrence rate of potential crop failure is greater than once every 4 years  
256 (25%). However, this function may be different in different parts of the world and different between crops (see  
257 Discussion).



258

259 **Figure 5: Membership function for climate variability showing the impact of the recurrence rate of potential crop failures on**  
 260 **crop suitability.** The seasonal recurrence rate is shown in percent.

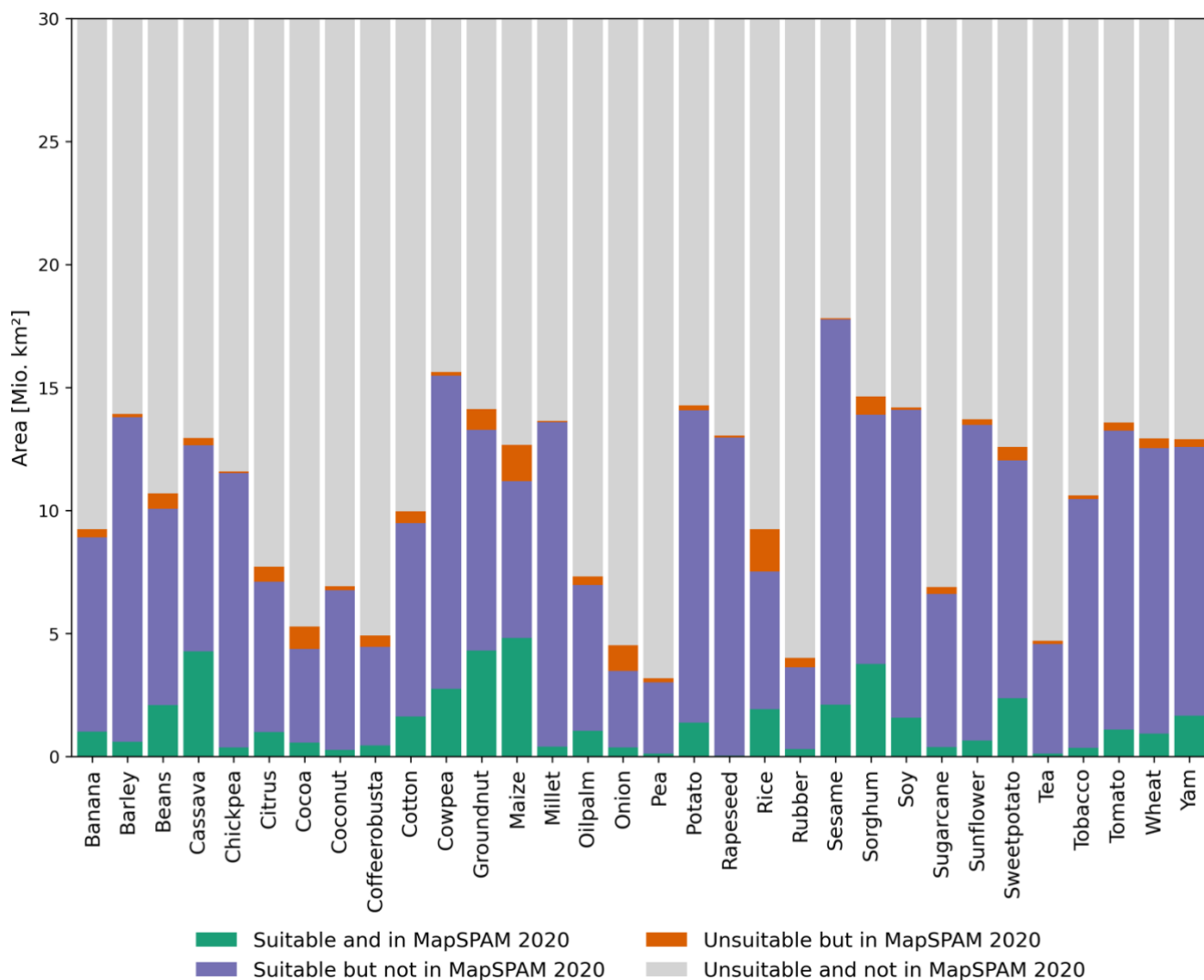
261 **3 Model evaluation**

262 Crop suitability is difficult to validate or measure, nor is it equivalent to agricultural yields or production values. However,  
 263 a comparison with other studies and data can provide valuable information and build confidence in the approach.

264 **3.1 Comparison with Harvested Area**

265 In principle, a crop should be suitable where it is already cultivated. According to this premise, we compare the suitable  
 266 area simulated with CropSuite with the harvested areas from the global spatially-disaggregated crop production statistics  
 267 data for 2020 (MapSPAM 2020 v1.0) produced by the International Food Policy Research Institute (IFPRI) using the  
 268 Spatial Production Allocation Model (SPAM) (Ifpri, 2024). The CropSuite results for Africa consider climate variability  
 269 and are combined for irrigated and rainfed areas according to Meier et al. (2018). While MapSPAM relates to the year  
 270 2020, our simulations refer to the 1991-2010 time period, which could be a source of uncertainty. Nevertheless, we used  
 271 MapSPAM 2020 instead of other available versions of MapSPAM, since it includes 32 crops from our investigation and  
 272 is the latest released version of MapSPAM. A comparison between CropSuite and different MapSPAM versions is shown  
 273 exemplarily for maize in Fig. S2, revealing a considerably better fit with CropSuite in the MapSPAM 2020 version. For  
 274 comparison, harvested areas below 10 ha per pixel are excluded from the calculation and the high spatial resolution of  
 275 the CropSuite model output is resampled to the same spatial resolution (5 arc minutes) than the MapSPAM 2020 data.  
 276 Figure 6 depicts the results of this analysis for all crops, where green and purple bars represent areas that are suitable,  
 277 while orange and green areas represent harvested areas in MapSPAM. Purple bars indicate suitable areas that are currently  
 278 not used by the respective crop. While green areas are also identified as being suitable in our approach, orange areas are

279 not suitable in CropSuite despite the respective crop is harvested according to MapSPAM. Crops with the largest  
 280 mismatching areas are rice, maize, and onion (Fig. 6). Most crops show a small proportion of orange to green areas,  
 281 except for onions, rapeseed, cocoa, pea, rubber, tea, coffee, and rice (Fig. S3). This can have various causes, such as data  
 282 uncertainty of climate, soil and irrigation data (Avellan et al., 2012), incorrect membership functions, the use of different  
 283 crop varieties, or an incorrect localization of the cultivation areas in MapSPAM due to high uncertainties in the underlying  
 284 national statistical data, especially in African countries (Yu et al., 2020), or applied crop management practices that could  
 285 level out ecological limitations.



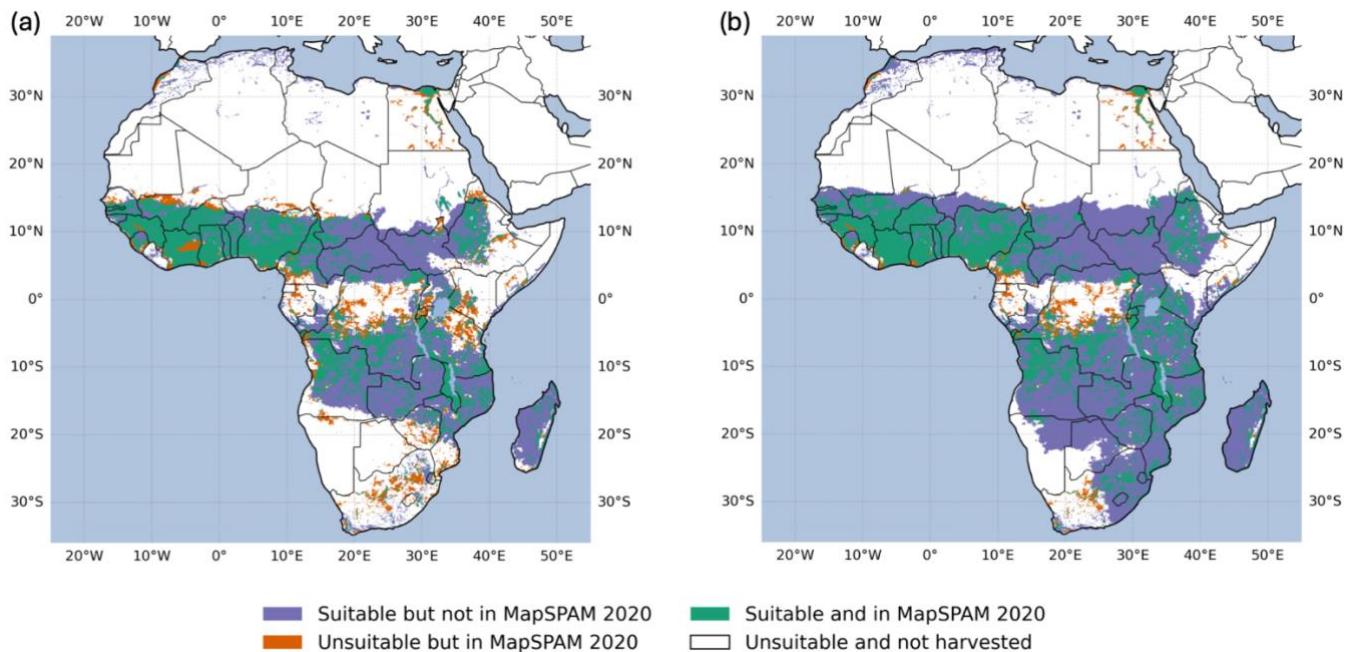
286

287 **Figure 6: Comparison of CropSuite with MapSPAM 2020 for all matching crops.** CropSuite results combine irrigated and rainfed  
 288 areas according to Meier et al. (2018) and consider climate variability. Areas on which the respective crop is harvested according to  
 289 MapSPAM and which are suitable according to CropSuite are shown in green, areas that are suitable but on which the crop is not

290 harvested are shown in purple. Areas that are unsuitable but are harvested according to MapSPAM are shown in orange, while  
291 unsuitable areas that are not harvested according to MapSPAM are shown in gray.

292 Figure 7a shows the spatial comparison between crop suitability and harvested areas for maize. Areas where maize is  
293 harvested according to MapSPAM, although CropSuite has identified these areas as unsuitable, are found mainly in  
294 Egypt, the northern Sahel, the Congo Basin, as well as parts of Cameroon, Gabon, Kenya, Tanzania, Zimbabwe and  
295 South Africa. Figure 7b shows the comparison ignoring the impact of climate variability on crop suitability. Disregarding  
296 climate variability results in large (blue) areas, which are considered suitable but are no harvest areas according to  
297 MapSPAM, especially along the dry belts (15°N and 20°S). Our approach considering climate variability (Fig. 7a)  
298 reduces these blue areas, but induces some mismatches, where MapSPAM indicates harvested areas and CropSuite shows  
299 no suitability (red areas). We find that the mismatching areas along the dry belts (including the Sahel) and in eastern  
300 Africa (Tanzania, Kenya) are often associated with limits due to climate variability. This indicates that the thresholds for  
301 climate variability (section 2.2) and the membership function (Fig. 5) might be parameterized slightly too exclusive.  
302 However, some of these regions might be used as cropland by smallholders or subsistence farmers despite the high risk  
303 of crop failures.

304 While in the inner tropics, the reason for limited crop suitability can primarily be attributed to soil acidity (pH), indicating  
305 possible uncertainties with used SoilGrids dataset, differences in Egypt mainly result from discrepancies according to  
306 different assumptions on irrigated areas.



307  
308 **Figure 7: Comparison of CropSuite with MapSPAM 2020 for maize.** (a) shows the comparison with consideration of climate  
309 variability in CropSuite, while climate variability is not considered in (b). Areas on which the respective crop is harvested according  
310 to MapSPAM and which are suitable according to CropSuite are shown in green, areas that are suitable but on which the crop is not

311 harvested are shown in blue. Areas that are not suitable but are harvested according to MapSPAM are shown in red. Unsuitable areas  
312 that are not harvested according to MapSPAM are shown in white.

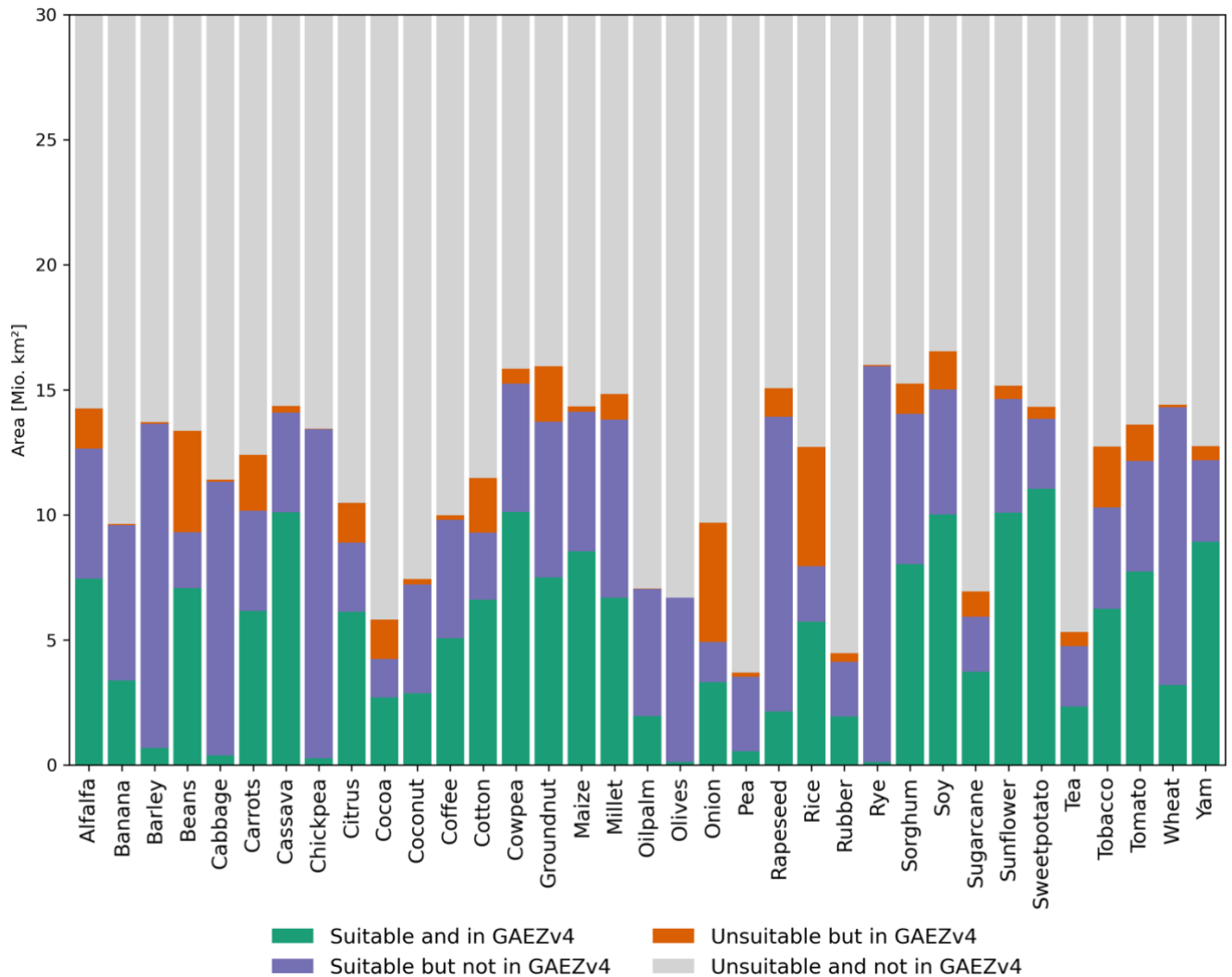
### 313 **3.2 Comparison with GAEZ**

314 A state-of-the-art climate-edaphic suitability assessment for crops is provided by the Global Agro-Ecological Zones  
315 (GAEZ) v4 (Fischer et al., 2021). For comparison with CropSuite, we used GAEZ data for the time period 1981-2010  
316 for high input level, rainfed conditions and the option ‘all land in grid cell’. The high input level refers to advanced  
317 management assumptions (fully mechanized, optimum application of nutrients and chemical pest, disease and weed  
318 control) (Fischer et al., 2021), which correspond best to the assumptions made in CropSuite for this study. The suitability  
319 range of the GAEZ data is transformed to the classification system as shown in Table 3. The CropSuite data for rainfed  
320 conditions is resampled (using the average) to the same spatial resolution of 5 arc minutes than the GAEZ data. For this  
321 comparison, we use CropSuite data without climate variability, since the GAEZ approach does not consider climate  
322 variability as well. Coffee was compared against the best type of robusta and arabica, as done in the GAEZ data (Fischer  
323 et al., 2021).

324 Overall, there are large overlaps between the GAEZ and CropSuite (Fig. 8). Generally, CropSuite identifies larger suitable  
325 areas than GAEZ for Africa (purple bar in Fig. 8), particularly for barley, cabbage, chickpea, rapeseed, rye and wheat. A  
326 main reason for differences may be due to different underlying soil data, GAEZ uses the HWSD while CropSuite uses



327 the SoilGrids data. The consideration of climate variability in CropSuite mainly results in larger areas that are unsuitable  
 328 in CropSuite but still suitable in GAEZv4 (orange bars) (Fig. S4).

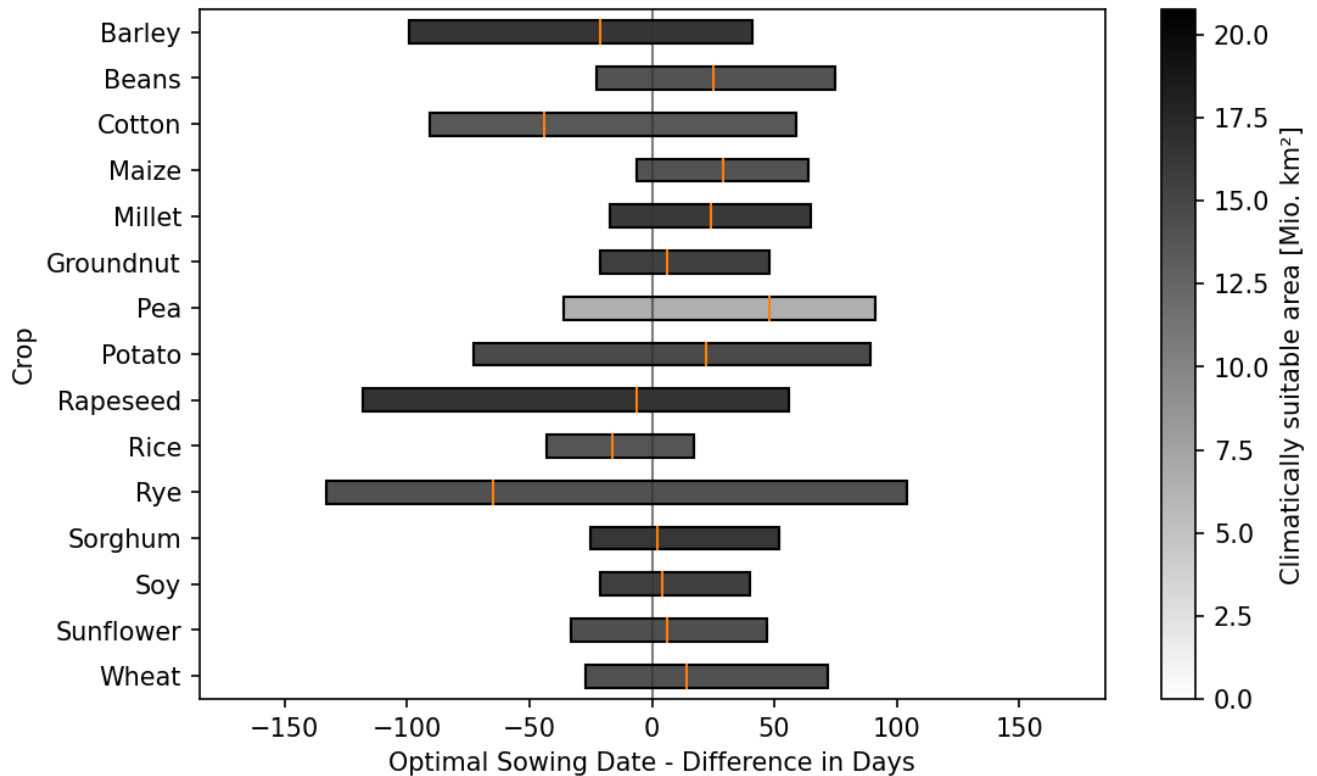


329  
 330 **Figure 8: Comparison between CropSuite and GAEZv4 suitability data for all matching crops.** CropSuite results are shown  
 331 without consideration of climate variability. Areas that are suitable in both data, CropSuite and GAEZv4 are shown in green, areas  
 332 suitable in CropSuite but not suitable in GAEZv4 are shown in purple. Unsuitable area in CropSuite that is suitable in GAEZv4 is  
 333 shown in orange. Areas that are unsuitable in both data are shown in grey.

### 334 3.3 Comparison of Optimal Sowing Dates with the GGCM Crop Calendar

335 Another method of validation involves comparing the optimal sowing dates computed with CropSuite with the crop  
 336 calendar from the Global Gridded Crop Model Intercomparison (GGCM), which is available globally for a variety of  
 337 different crops at half degree spatial resolution (Jägermeyr et al., 2021). Figure 9 illustrates the average differences of the

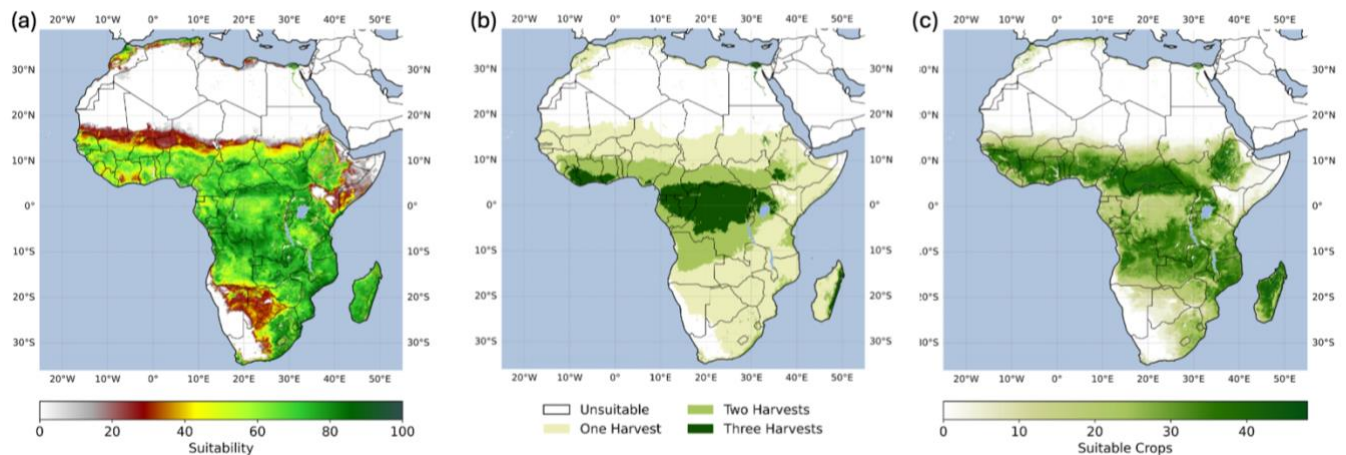
338 sowing dates across Africa, averaged for the matching crops between the two datasets. The comparison is performed at  
 339 a spatial resolution of 30 arc seconds (Fig. 9) and at half degree resolution (see Fig. S5). For the high spatial resolution,  
 340 the GGCM data are interpolated to 30 arc seconds using nearest neighbor. Unlike CropSuite, which displays the optimal  
 341 sowing date, the GGCM data show the actual sowing date based on extrapolated statistics. Thus, there might be  
 342 differences between the optimal and actual sowing dates. It must also be considered that the GGCM crop calendar is  
 343 based on statistics that apply to discrete areas at relatively coarse half degree spatial resolution, while CropSuite was  
 344 simulated at a pixel accuracy of 30 arc seconds spatial resolution. In fact, the median differences are mostly within one  
 345 month of the GGCM crop calendar, which generally indicates a high agreement. At the coarse resolution, the difference  
 346 between the two datasets is less and the spread is smaller (Fig. S5).



347  
 348 **Figure 9: Comparison of the optimal sowing dates of CropSuite with the actual sowing dates of the GGCM crop calendars.**  
 349 The area-weighted shift of the sowing date in days is shown for all matching crops. Negative values mean an earlier sowing date in  
 350 CropSuite, positive values mean a later sowing date in CropSuite compared to the GGCM Crop Calendar. The bars show the 5th and  
 351 95th percentile, the orange marker shows the median. The color of the bars indicates the climatically suitable area for the whole of  
 352 Africa. Irrigated areas are considered according to Meier et al. (2018). The comparison is performed at 30 arc seconds spatial resolution  
 353 for both datasets.

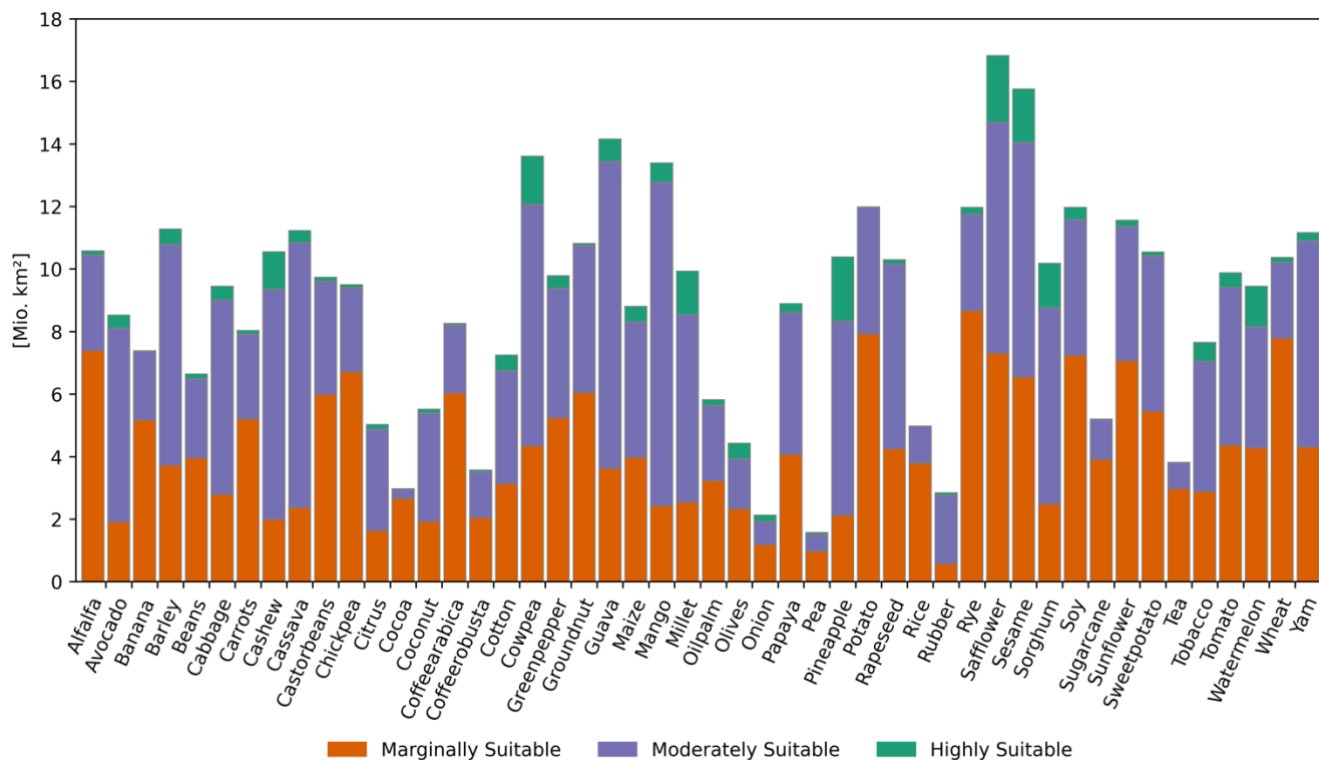
#### 354 4 Simulation Results

355 Crop suitability is simulated for historical climate conditions (1991-2010) for rainfed and irrigated conditions. Figure 10a  
356 illustrates the overall crop suitability, showing for each location the value for the most suitable of all considered crops.  
357 Irrigation is considered according to the currently irrigated areas for Africa (Meier et al., 2018), such as along the Nile  
358 river in Egypt (see Fig. S1 for irrigated areas in Africa). In total for Africa, 5.7 million km<sup>2</sup> are highly suitable, 10.6  
359 million km<sup>2</sup> are moderately suitable, 3.3 million km<sup>2</sup> are marginally suitable and 10.4 million km<sup>2</sup> are not suitable for  
360 crop cultivation. Mainly between 10° N and 10° S, a high potential for multiple cropping exists with the possibility of  
361 two or three harvests per year (Fig. 10b). Looking at the number of crops suitable for cultivation (Fig. 10c), a large  
362 proportion of the considered crops can grow particularly along the wet savannahs, which gives these regions plenty of  
363 opportunities for cultivation. In contrast, only a few crops are suitable for the inner tropics and the dry savannahs, which  
364 limits the possibilities for switching between crops.



365 **Figure 10: (a) Overall crop suitability, (b) potential multiple cropping, and (c) number of suitable crops under historical climate**  
366 **conditions from 1991 to 2010.** Irrigated areas are considered according to Meier et al. (2018). The overall crop suitability (a) and the  
367 potential multiple cropping (b) are each shown for the most suitable crop at each location. The maximal number of suitable crops  
368 results from the number of 48 considered crops (see Table 1).  
369

370 Figure 11 shows the suitable area for each of the simulated crops for Africa. The five crops with the largest suitable areas  
371 in Africa are safflower (16.82 mio km<sup>2</sup>), sesame (15.76), guava (14.15), cowpea (13.61), and mango (13.39).



372

373

374

**Figure 11: Marginally, moderately and highly suitable areas for all 48 crops under historical climate conditions from 1991 to 2010 for Africa.** Suitability classes are chosen according to Table 3. Irrigated areas are considered according to Meier et al. (2018).

375

376

377

378

379

380

381

382

383

384

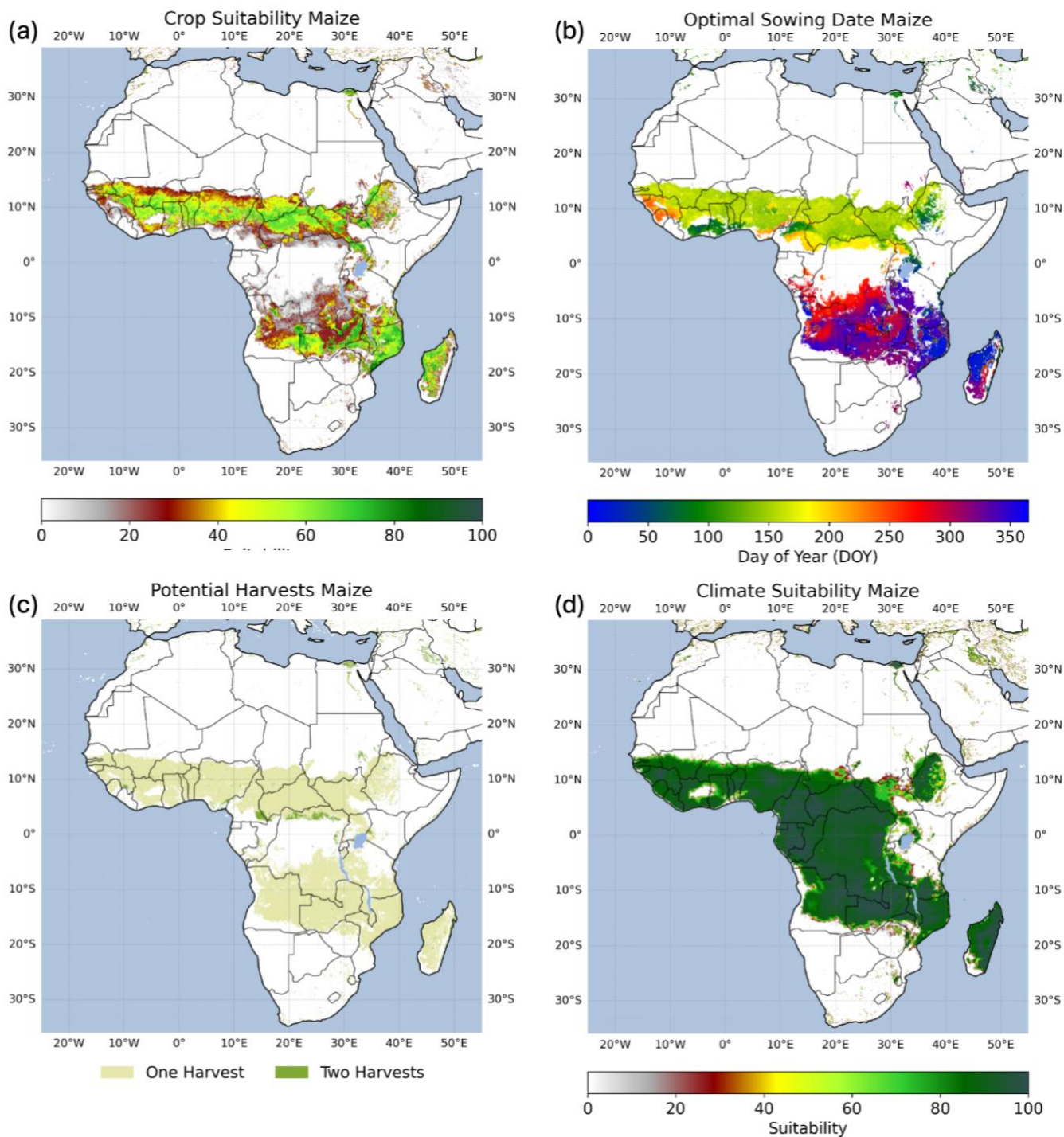
385

386

Figure 12a exemplarily shows the crop suitability simulated for maize. The maps for all crops are provided via Zenodo (see Data Availability). Maize is highly suitable along a strip of the 10° N and the 20° S parallel as well as large parts of Mozambique and Madagascar. In total, 0.49 million km<sup>2</sup> are highly suitable, 4.34 million km<sup>2</sup> are moderately suitable, 3.97 million km<sup>2</sup> are marginally suitable and 21.23 million km<sup>2</sup> are unsuitable.

The optimal sowing date for single cropping (Fig. 12b) for maize shifts with latitude from the northern hemisphere across the equator to the southern hemisphere. Figure 12c shows the potential number of potential harvests per year for maize. Climate conditions allow up to two harvests per year in some parts of Congo and Cameroon and in the irrigated areas e.g. along the Nile river. Optimal sowing dates for first and second sowing on areas suitable for multiple cropping are shown in Fig. S6.

Figure 12d shows the climate suitability for maize, which just considers climatic constraints for the suitability of maize. In comparison to the crop suitability map (Fig. 12a), more areas are suitable and suitability is substantially higher, if soil and topography are not considered and therefore do not limit or reduce crop suitability.



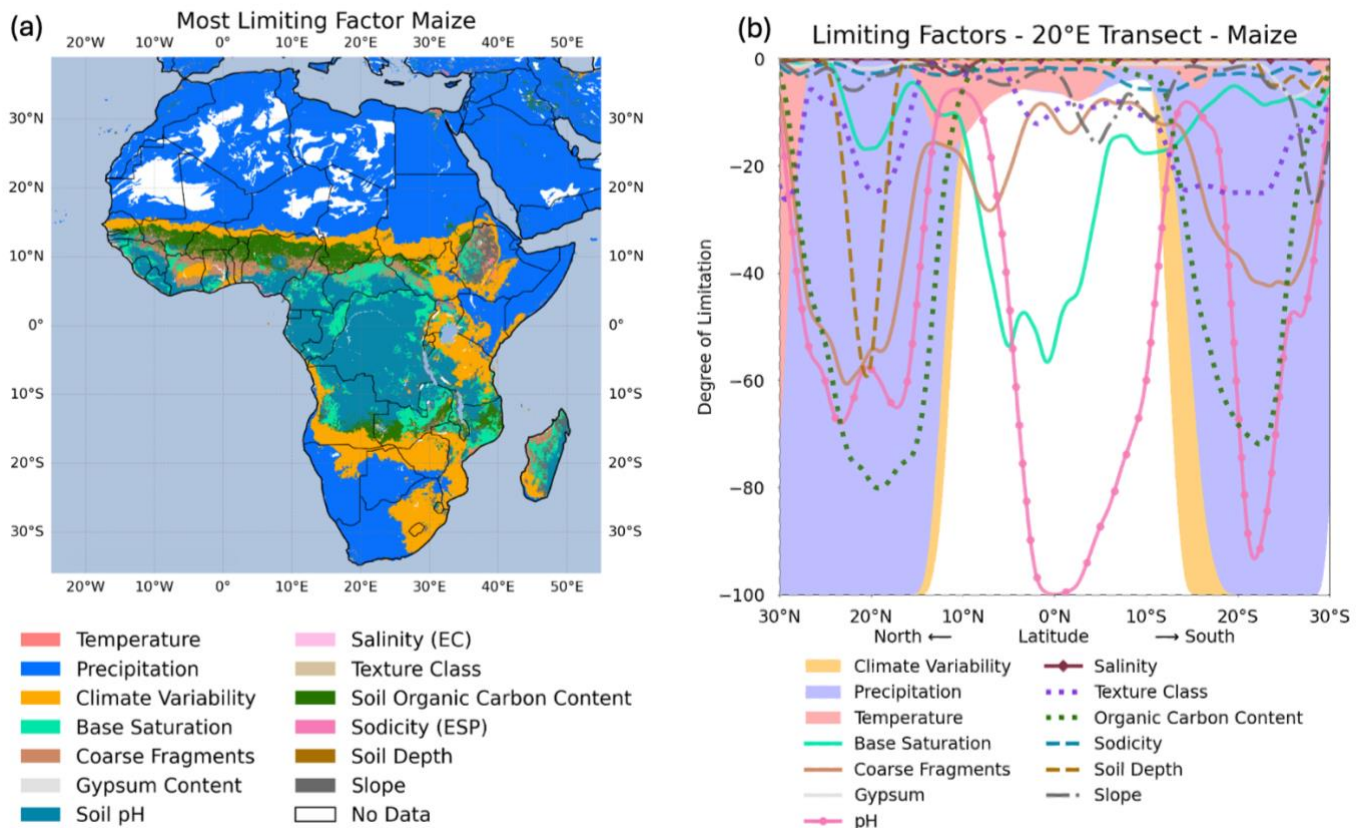
387

388 **Figure 12: (a) Crop suitability, (b) optimal sowing date for single cropping, (c) potential multiple cropping, and (d) climate**  
 389 **suitability for maize under historical climate conditions from 1991 to 2010. Irrigated areas are considered according to Meier et**  
 390 **al. (2018).**

391 The most limiting factor is shown in Fig. 13a. While low precipitation prevents maize from being suitable in large parts  
392 of Africa in the arid deserts, soil is predominantly restricting suitability in tropical regions. Particularly pH is the most  
393 limiting factor in the humid tropics, such as the Congo Basin, where soils are too acid for growing maize. A large band  
394 along the drylands highlights regions where inter-annual climate variability is most limiting maize suitability (in orange,  
395 Fig. 13a). Here, climate conditions are instable for maize cultivation, and the recurrence rate of potential crop failures is  
396 larger than 25% (every fourth year). For maize, climate variability is limiting crop suitability on 4.4 million km<sup>2</sup> for  
397 Africa (Fig 13a).

398 Figure 13b shows the degree of limitation for all considered climate, soil and terrain factors along a transect following  
399 the 20° E from North to South. In the Sahara, several factors, including temperature, organic carbon content, and soil pH,  
400 are not in an optimal range, while precipitation and the climate variability are the most limiting (note that climate  
401 variability is by definition a limiting factor if precipitation and/or temperature are limiting factors). Due to the unfavorable  
402 soil conditions, irrigation would only slightly improve maize suitability here. Between 15° N and 5° N, the limitations of  
403 all factors are relatively low. Here, coarse fragments and base saturation are most limiting. The tropical areas along the  
404 transect between 5° N and 10° S are mainly constrained by soil pH. Accordingly, soil management or practices that  
405 increase pH in these regions would have a significantly positive impact on crop suitability in this region, since no other  
406 factor has such a strong impact on maize suitability. Further south, low precipitation again mostly limits maize suitability.





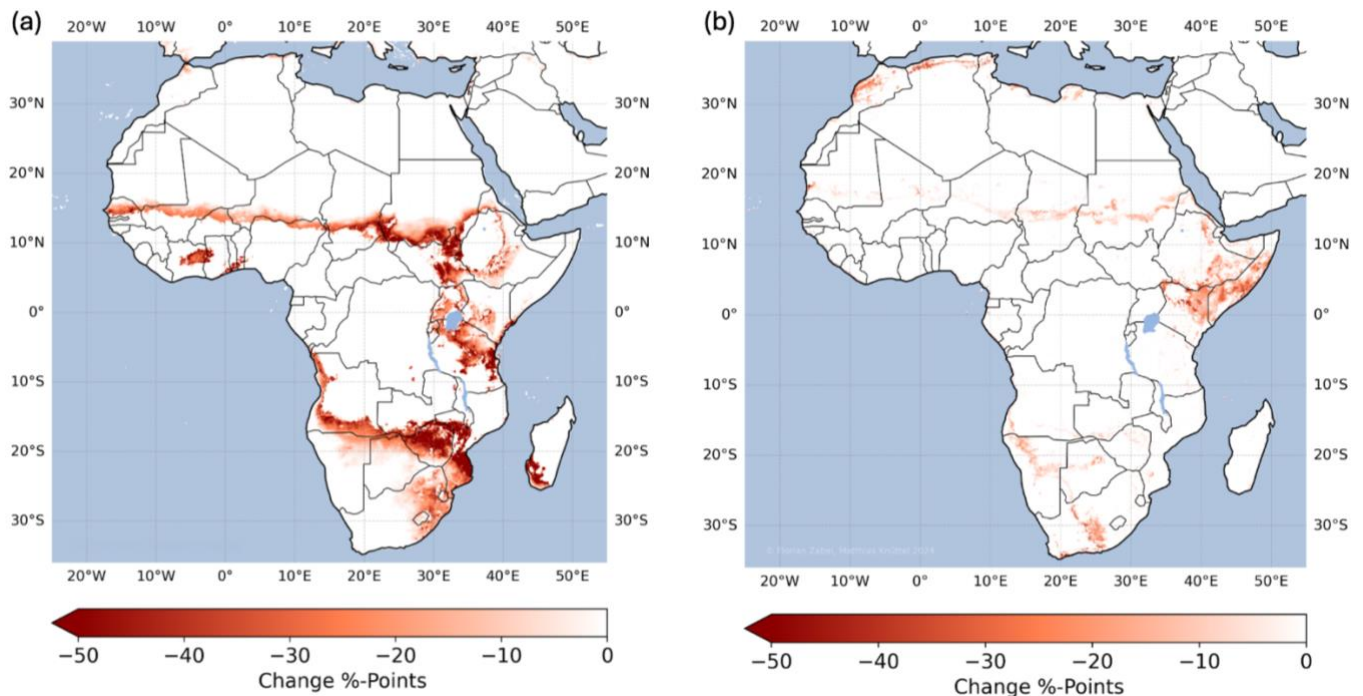
407

408 **Figure 13: Limiting factors.** (a) Most limiting factor of the crop suitability for maize under historical climate conditions from 1991  
 409 to 2010. (b) shows the degree of limitation of all factors along a transect of the 20° East from 30° North to 30° South. The most limiting  
 410 factors are displayed with priority according to the order in the legend in (a), if more than one factor fully limits the suitability. For  
 411 visualization, the shapes in (b) are smoothed using a moving average. Irrigated areas are considered according to Meier et al. (2018)  
 412 in (a) and are not considered in (b).

413 The consideration of climate variability significantly reduces climate suitability for maize as shown in Fig. 14a, mainly  
 414 in the transition area between dry savannah and desert in the Sahel zone, in Burundi and Tanzania in Eastern Africa, and  
 415 in the southern part of Africa in Angola, Zambia, Zimbabwe, Mozambique, South Africa, and the southern part of  
 416 Madagascar. In total, climate variability reduces climate suitability on more than 5.4 million km<sup>2</sup>.

417 Optimal sowing dates also shift when considering climate variability, since the algorithm identifies the best suitable time  
 418 window for the growing cycle over the year (Fig. S7). As a result, optimal sowing for maize considerably shifts in  
 419 Tanzania, Mozambique and Madagascar.

420 Over all crops, Fig. 14b shows the impact of climate variability on the overall crop suitability. In this case, overall crop  
 421 suitability is reduced on 2.2 million km<sup>2</sup>, mainly reduced in Somalia, Kenya, Ethiopia, South Africa, and the Maghreb  
 422 countries of Morocco, Algeria, Tunisia, and Libya. These regions generally show a high vulnerability to climatic  
 423 variability. Climate variability also reduces the potential for multiple cropping in general over all crops on more than 2.3  
 424 million km<sup>2</sup> (Fig. S8).



425

426

427

**Figure 14: Impact of the consideration of climate variability on crop suitability (a) for maize (b) for the overall crop suitability of all crops under historical climate conditions from 1991 to 2010. Irrigated areas are considered according to Meier et al. (2018).**

428

## 5 Discussion

429

430

431

432

433

434

435

436

437

438

439

440

441

442

We found that the consideration of climate variability significantly affects crop suitability, multiple cropping, and optimal sowing dates in Africa. Our approach allows to adjust the risk aversion of farmers by adjusting the thresholds for climate variability (section 2.2.) and the membership function (Fig. 5). The shape of this function may differ between crops and regions and might be influenced by several socio-economic factors, such as the degree of mechanization, financial possibilities, and the availability of crop insurances, which is likely to reduce risk aversion of farmers. We suggest the function as shown in Fig. 5 as a broad and general solution which is primarily designed to represent risk aversion of commercial farms. In our comparison analysis for maize (section 3), reference data showed some cultivation in the regions we identified as unsuitable due to the high recurrence rate of potential crop failures caused by high climate variability (Fig. 7). In some regions, despite the high risk of crop failures, land might be cultivated by smallholders or subsistence farmers that have no other choice but to cultivate these lands. However, we admit that the tuning of the climate variability thresholds and the membership function requires more research, and the optimal results will vary depending on crop and region. CropSuite offers the platform and the possibilities to conduct such assessments. The results of CropSuite (section 4) are subject to uncertainties in the applied climate, soil, terrain, and irrigation data as well as the membership functions (Fig. 1). Soil and terrain data are assumed to be static, although management could



443 influence soil properties such as pH, and terracing could reduce slope limitations. The applied climate data from CHIRPS  
444 and CHIRTS are found to be particularly valuable in regions, where climate stations are sparse. Over Africa, CHIRPS is  
445 successfully validated (Dinku et al., 2018) showing good performance (Lemma et al., 2019; Muthoni et al., 2019). Verdin  
446 et al. (2020) also report good agreement of CHIRTS over Africa, however with a poor performance over central Africa,  
447 the Horn of Africa, and parts of northern Mali. Generally, both data sets rely on station data to correct the satellite  
448 estimations, which is why uncertainties for very data-scarce regions remain. To apply CropSuite in regions outside 50°S-  
449 50°N, or to larger time periods before the 1980s, the user of CropSuite could also rely on global high-resolution climate  
450 reanalysis, such as ERA5 (Hersbach et al., 2020). For the African continent, ERA5 reanalysis shows large improvements  
451 over its predecessor ERA-Interim (Gleixner et al., 2020). Still, considerable deviations in precipitation from CHIRPS are  
452 reported, e.g., wet biases over Uganda (Gleixner et al., 2020) and a dry bias over the western Sahel (Gbode et al., 2023),  
453 where CHIRPS is applied as reference. We therefore assume that CHIRPS and CHIRTS are very suitable climatic data  
454 sets to investigate our example of maize suitability in Africa. The soil profiles used for the generation of the SoilGrids  
455 show a heterogeneous distribution, with large gaps over central Africa, which is why Hengl et al. (2017) attribute  
456 uncertainty in the data to the under-sampling. They argue that a few hundred additional profiles in under-sampled areas  
457 could massively improve the resulting SoilGrids.

458 The membership functions derived by Sys et al. (1993) are widely applied but are also governed by inherent uncertainties.  
459 Herzberg et al. (2019) argue that the assessment by Sys et al. (1993) is not detailed enough to capture specific features of  
460 small areas. They find that Sys et al. (1993) would consider a hilly area in tropical Vietnam unsuitable due to too acidic  
461 soils and steep slopes, whereas the local farmers can cultivate the land. Furthermore, the approach cannot account for  
462 compound effects and interactions of the climate and soil variables (Elsheikh et al., 2013). The membership functions  
463 cover the general behavior in a univariate manner, while the real plant physiology is a more complex interplay of climatic  
464 variables and soil conditions (Joswig et al., 2022). This also applies particularly to compound extremes, for example the  
465 combination of hot and dry climatic conditions (Goulart et al., 2023) that limit water availability and favor evaporation,  
466 which can trigger water and temperature stress in plants. This is relevant in the course of a warming climate, as the joint  
467 probability of hot and dry conditions is projected to increase in many regions of the world (Bevacqua et al., 2022; Felsche  
468 et al., 2024). This is however no specific drawback of CropSuite, but rather a lack of bivariate, multivariate or interactive  
469 membership functions. The assessment of the membership functions by Sys et al. (1993) is also outdated for new crop  
470 varieties that might be more resilient to climatic and environmental stressors (Peter et al., 2020). Furthermore, we argue  
471 that the uncertainty in the temperature and precipitation membership functions is by design larger at its low and high  
472 ends, as the functions are derived empirically. Since our consideration of climate variability is based on the 5% to 10%  
473 suitability values, respectively (see Section 2.2), the uncertainties of the membership functions are propagated to the  
474 assessment of climate variability. More research and updated functions could support the results by CropSuite.

475 The sampling of climate variability within 20-year periods is limited as variability can cover wide time ranges. There,  
476 the application of single-model initial condition large ensembles can help to robustly assess the variability based on

477 decadal or multidecadal time periods (Deser et al., 2020). This is especially important for precipitation and precipitation  
478 extremes, which show a high sensitivity to climate variability (Lang and Poschlod, 2024; Tebaldi et al., 2021).  
479 Furthermore, for the assessment of climate variability, we only capture the occurrence of growing seasons exceeding the  
480 percentile thresholds, but we do not consider the intensity of the according events. Single days with extreme precipitation  
481 can induce flooding that leads to crop failures (Balgah et al., 2023; Müller et al., 2023), even though the average  
482 precipitation for the growing season is still within the suitable range of the membership function. This drawback however  
483 also applies for most of the mechanistic crop models at global scale (Ruane et al., 2017), while regional applications  
484 evolve incorporating crop losses due to waterlogging and flooding (Li et al., 2016; Monteleone et al., 2023; Pasley et al.,  
485 2020). This is why we claim to assess climate variability not climate extremes inducing potential crop failures.

## 486 **6 Conclusions**

487 CropSuite is a new easy-to-use comprehensive open-source model that provides a complete processing chain  
488 (preprocessing, spatial downscaling, suitability simulations, data analysis and visualization) for carrying out crop  
489 suitability and climate change impact analysis. CropSuite allows users to easily parameterize different varieties of the  
490 same crops or additional crops by determining the membership functions in the GUI. Thereby, the fuzzy logic approach  
491 makes it easy to use expert knowledge for the parameterization of the membership functions. Besides all data and  
492 compiled maps generated, we provide a user manual for CropSuite (Zabel and Knüttel, 2024) and the parameterizations  
493 of the considered 48 crops in this study. Furthermore, the model allows the flexible addition of further parameters and  
494 membership functions that might affect suitability, if the required data is provided. For the future, this allows the  
495 consideration of further ecological and socio-economic limitations (such as access to fertilizers, available labor, know-  
496 how, infrastructure and transportation, heat stress impacts on labor) that have not yet been sufficiently considered in crop  
497 suitability assessments (Orlov et al., 2024; Akpoti et al., 2019).

498 For this study, we simulated 48 crops for Africa under the consideration of climate variability for historical climate  
499 conditions. Thus, we created a huge dataset, providing detailed high-resolution information on climate-, soil-, and crop  
500 suitability, optimal sowing dates, multiple cropping potentials and the limiting factors, which can be used for follow-up  
501 studies and climate impact assessments. Additionally, the data include substantial information to develop strategies for  
502 an efficient land-use (Schneider et al., 2024; Molina Bacca et al., 2023; Delzeit et al., 2019). The consideration of future  
503 climate change scenarios will allow for investigating efficient strategies for climate change adaptation through shifting  
504 sowing dates, or cultivar and land-use change. Further, information about the limiting factors can be helpful to optimize  
505 crop management, since it identifies the parameter that most efficiently improves crop suitability.

506 **Code Availability**

507 CropSuite (v1.0) code is written in Python and is available Open-Source (CC BY-SA 4.0) together with the GUI at  
508 Zenodo (<https://doi.org/10.5281/zenodo.14259375>) and GitHub (<https://github.com/flozabel/CropSuite>). A user manual  
509 is provided separately via Zenodo (<https://doi.org/10.5281/zenodo.14196315>).

510 **Data Availability**

511 The resulting data are available for download as GeoTIFF files via Zenodo (<https://doi.org/10.5281/zenodo.14196331>).  
512 In addition to the figures shown as examples for maize in this paper, the compiled figures for all 48 considered crops are  
513 provided for download, including a separation of rainfed and irrigated agricultural systems and a comparison with  
514 MapSPAM 2020 (<https://doi.org/10.5281/zenodo.14196331>).

515 **Author contribution**

516 FZ conceptualized and developed the model. MK programmed the CropSuite model and the GUI in Python. FZ, MK,  
517 and BP developed the methodology for the consideration of climate variability. FZ and MK performed the simulations  
518 and analyzed the results. FZ and MK prepared the manuscript with contributions from BP.

519 **Competing interests**

520 The authors declare that they have no conflict of interest.

521 **Acknowledgements**

522 The simulations were performed at sciCORE (<http://scicore.unibas.ch/>) scientific computing center at University of  
523 Basel, requiring in total approximately 150.000 CPUh. We thank CGIAR and CIAT for their support and the scholarship  
524 provided to MK and the collaboration for the Africa Agriculture Adaptation Atlas.

525 **References**

526 Abdulai, A. L., Kouressy, M., Vaksmann, M., Asch, F., Giese, M., and Holger, B.: Latitude and Date of Sowing  
527 Influences Phenology of Photoperiod-Sensitive Sorghums, *Journal of Agronomy and Crop Science*, 198, 340-348,  
528 10.1111/j.1439-037X.2012.00523.x, 2012.  
529 Akpoti, K., Kabo-bah, A. T., and Zwart, S. J.: Review - Agricultural land suitability analysis: State-of-the-art and outlooks  
530 for integration of climate change analysis, *Agricultural Systems*, 173, 172-208,  
531 <https://doi.org/10.1016/j.agsy.2019.02.013>, 2019.

532 Akpoti, K., Kabo-bah, A. T., Dossou-Yovo, E. R., Groen, T. A., and Zwart, S. J.: Mapping suitability for rice production  
533 in inland valley landscapes in Benin and Togo using environmental niche modeling, *Science of The Total*  
534 *Environment*, 709, 136165, <https://doi.org/10.1016/j.scitotenv.2019.136165>, 2020.

535 Asseng, S., Spänkuch, D., Hernandez-Ochoa, I. M., and Laporta, J.: The upper temperature thresholds of life, *The Lancet*  
536 *Planetary Health*, 5, e378-e385, [https://doi.org/10.1016/S2542-5196\(21\)00079-6](https://doi.org/10.1016/S2542-5196(21)00079-6), 2021.

537 Avellan, T., Zabel, F., and Mauser, W.: The influence of input data quality in determining areas suitable for crop growth  
538 at the global scale – a comparative analysis of two soil and climate datasets, *Soil Use and Management*, 28, 249-265,  
539 <https://doi.org/10.1111/j.1475-2743.2012.00400.x>, 2012.

540 Balgah, R. A., Ngwa, K. A., Buchenrieder, G. R., and Kimengsi, J. N.: Impacts of Floods on Agriculture-Dependent  
541 Livelihoods in Sub-Saharan Africa: An Assessment from Multiple Geo-Ecological Zones, *Land*, 12, 334, 2023.

542 Batjes, N. H.: Harmonized soil property values for broad-scale modelling (WISE30sec) with estimates of global soil  
543 carbon stocks, *Geoderma*, 269, 61-68, <https://doi.org/10.1016/j.geoderma.2016.01.034>, 2016.

544 Bevacqua, E., Zappa, G., Lehner, F., and Zscheischler, J.: Precipitation trends determine future occurrences of compound  
545 hot-dry events, *Nat Clim Change*, 12, 350-355, 10.1038/s41558-022-01309-5, 2022.

546 Bonfante, A., Monaco, E., Alfieri, S. M., De Lorenzi, F., Manna, P., Basile, A., and Bouma, J.: Chapter Two - Climate  
547 Change Effects on the Suitability of an Agricultural Area to Maize Cultivation: Application of a New Hybrid Land  
548 Evaluation System, in: *Advances in Agronomy*, edited by: Sparks, D. L., Academic Press, 33-69,  
549 <https://doi.org/10.1016/bs.agron.2015.05.001>, 2015.

550 Chapman, S., E Birch, C., Pope, E., Sallu, S., Bradshaw, C., Davie, J., and H Marsham, J.: Impact of climate change on  
551 crop suitability in sub-Saharan Africa in parameterized and convection-permitting regional climate models,  
552 *Environmental Research Letters*, 15, 094086, 10.1088/1748-9326/ab9daf, 2020.

553 Chemura, A., Gleixner, S., and Gornott, C.: Dataset of the suitability of major food crops in Africa under climate change,  
554 *Scientific Data*, 11, 294, 10.1038/s41597-024-03118-1, 2024.

555 Chen, D., Dai, A., and Hall, A.: The Convective-To-Total Precipitation Ratio and the “Drizzling” Bias in Climate Models,  
556 *Journal of Geophysical Research: Atmospheres*, 126, e2020JD034198, <https://doi.org/10.1029/2020JD034198>, 2021.

557 Cober, E. R. and Morrison, M. J.: Regulation of seed yield and agronomic characters by photoperiod sensitivity and  
558 growth habit genes in soybean, *Theoretical and Applied Genetics*, 120, 1005-1012, 10.1007/s00122-009-1228-6,  
559 2010.

560 Cronin, J., Zabel, F., Dessens, O., and Anandarajah, G.: Land suitability for energy crops under scenarios of climate  
561 change and land-use, *GCB Bioenergy*, 12, 648–665-648–665, <https://doi.org/10.1111/gcbb.12697>, 2020.

562 Daly, C., Neilson, R. P., and Phillips, D. L.: A Statistical-Topographic Model for Mapping Climatological Precipitation  
563 over Mountainous Terrain, *Journal of Applied Meteorology and Climatology*, 33, 140-158,  
564 [https://doi.org/10.1175/1520-0450\(1994\)033<0140:ASTMFM>2.0.CO;2](https://doi.org/10.1175/1520-0450(1994)033<0140:ASTMFM>2.0.CO;2), 1994.

565 Damiani, A., Ishizaki, N. N., Sasaki, H., Feron, S., and Cordero, R. R.: Exploring super-resolution spatial downscaling  
566 of several meteorological variables and potential applications for photovoltaic power, *Scientific Reports*, 14, 7254,  
567 10.1038/s41598-024-57759-8, 2024.

568 Delzeit, R., Pongratz, J., Schneider, J. M., Schuenemann, F., Mauser, W., and Zabel, F.: Forest restoration: Expanding  
569 agriculture, *Science*, 366, 316–317-316–317, <https://doi.org/10.1126/science.aaz0705>, 2019.

570 Deser, C., Lehner, F., Rodgers, K. B., Ault, T., Delworth, T. L., DiNezio, P. N., Fiore, A., Frankignoul, C., Fyfe, J. C.,  
571 Horton, D. E., Kay, J. E., Knutti, R., Lovenduski, N. S., Marotzke, J., McKinnon, K. A., Minobe, S., Randerson, J.,  
572 Screen, J. A., Simpson, I. R., and Ting, M.: Insights from Earth system model initial-condition large ensembles and  
573 future prospects, *Nat Clim Change*, 10, 277-286, 10.1038/s41558-020-0731-2, 2020.

574 Dinku, T., Funk, C., Peterson, P., Maidment, R., Tadesse, T., Gadain, H., and Ceccato, P.: Validation of the CHIRPS  
575 satellite rainfall estimates over eastern Africa, *Quarterly Journal of the Royal Meteorological Society*, 144, 292-312,  
576 <https://doi.org/10.1002/qj.3244>, 2018.

577 Elsheikh, R., Mohamed Shariff, A. R. B., Amiri, F., Ahmad, N. B., Balasundram, S. K., and Soom, M. A. M.: Agriculture  
578 Land Suitability Evaluator (ALSE): A decision and planning support tool for tropical and subtropical crops, *Comput*  
579 *Electron Agr*, 93, 98-110, <https://doi.org/10.1016/j.compag.2013.02.003>, 2013.

580 FAO: The Ecocrop Database [dataset], 2024.

581 FAO, IIASA, ISRIC, ISSCAS, and JRC: Harmonized World Soil Database (version 1.2) [dataset], 2012.

582 Farr, T. G., Rosen, P. A., Caro, E., Crippen, R., Duren, R., Hensley, S., Kobrick, M., Paller, M., Rodriguez, E., Roth, L.,  
583 Seal, D., Shaffer, S., Shimada, J., Umland, J., Werner, M., Oskin, M., Burbank, D., and Alsdorf, D.: The Shuttle  
584 Radar Topography Mission, *Reviews of Geophysics*, 45, RG2004, 10.1029/2005RG000183, 2007.

585 Felsche, E., Böhnisch, A., Poschlod, B., and Ludwig, R.: European hot and dry summers are projected to become more  
586 frequent and expand northwards, *Communications Earth & Environment*, 5, 410, 10.1038/s43247-024-01575-5,  
587 2024.

588 Fick, S. E. and Hijmans, R. J.: WorldClim 2: new 1-km spatial resolution climate surfaces for global land areas,  
589 *International Journal of Climatology*, 37, 4302-4315, 10.1002/joc.5086, 2017.

590 Fiddes, J., Aalstad, K., and Lehning, M.: TopoCLIM: rapid topography-based downscaling of regional climate model  
591 output in complex terrain v1.1, *Geosci. Model Dev.*, 15, 1753-1768, 10.5194/gmd-15-1753-2022, 2022.

592 Fischer, G., Nachtergaele, F. O., van Velthuizen, H. T., Chiozza, F., Franceschini, G., Henry, M., Muchoney, D., and  
593 Tramberend, S.: *Global Agro-Ecological Zones v4 - Model documentation*, 1, FAO, Rome,  
594 <https://doi.org/10.4060/cb4744en>, 2021.

595 Franke, J. A., Müller, C., Minoli, S., Elliott, J., Folberth, C., Gardner, C., Hank, T., Izaurralde, R. C., Jägermeyr, J., Jones,  
596 C. D., Liu, W., Olin, S., Pugh, T. A. M., Ruane, A. C., Stephens, H., Zabel, F., and Moyer, E. J.: Agricultural  
597 breadbaskets shift poleward given adaptive farmer behavior under climate change, *Global Change Biol*, 28, 167–181-  
598 167–181, <https://doi.org/10.1111/gcb.15868>, 2021.

599 Funk, C., Peterson, P., Landsfeld, M., Pedreros, D., Verdin, J., Shukla, S., Husak, G., Rowland, J., Harrison, L., Hoell,  
600 A., and Michaelsen, J.: The climate hazards infrared precipitation with stations—a new environmental record for  
601 monitoring extremes, *Scientific Data*, 2, 150066, 10.1038/sdata.2015.66, 2015.

602 Funk, C., Peterson, P., Peterson, S., Shukla, S., Davenport, F., Michaelsen, J., Knapp, K. R., Landsfeld, M., Husak, G.,  
603 Harrison, L., Rowland, J., Budde, M., Meiburg, A., Dinku, T., Pedreros, D., and Mata, N.: A High-Resolution 1983–  
604 2016 Tmax Climate Data Record Based on Infrared Temperatures and Stations by the Climate Hazard Center, *Journal*  
605 *of Climate*, 32, 5639-5658, <https://doi.org/10.1175/JCLI-D-18-0698.1>, 2019.

606 Gbode, I. E., Babalola, T. E., Diro, G. T., and Intsiful, J. D.: Assessment of ERA5 and ERA-Interim in Reproducing  
607 Mean and Extreme Climates over West Africa, *Advances in Atmospheric Sciences*, 40, 570-586, 10.1007/s00376-  
608 022-2161-8, 2023.

609 Gleixner, S., Demissie, T., and Diro, G. T.: Did ERA5 Improve Temperature and Precipitation Reanalysis over East  
610 Africa?, *Atmosphere*, 11, 996, 2020.

611 Goulart, H. M. D., van der Wiel, K., Folberth, C., Balkovic, J., and van den Hurk, B.: Storylines of weather-induced crop  
612 failure events under climate change, *Earth Syst. Dynam.*, 12, 1503-1527, 10.5194/esd-12-1503-2021, 2021.

613 Goulart, H. M. D., van der Wiel, K., Folberth, C., Boere, E., and van den Hurk, B.: Increase of Simultaneous Soybean  
614 Failures Due To Climate Change, *Earth's Future*, 11, e2022EF003106, <https://doi.org/10.1029/2022EF003106>, 2023.

615 Hengl, T., de Jesus, J. M., MacMillan, R. A., Batjes, N. H., Heuvelink, G. B. M., Ribeiro, E., Samuel-Rosa, A., Kempen,  
616 B., Leenaars, J. G. B., Walsh, M. G., and Gonzalez, M. R.: SoilGrids1km — Global Soil Information Based on  
617 Automated Mapping, *PLOS ONE*, 9, e105992, 10.1371/journal.pone.0105992, 2014.

618 Hengl, T., Mendes de Jesus, J., Heuvelink, G. B. M., Ruiperez Gonzalez, M., Kilibarda, M., Blagotić, A., Shangguan,  
619 W., Wright, M. N., Geng, X., Bauer-Marschallinger, B., Guevara, M. A., Vargas, R., MacMillan, R. A., Batjes, N.  
620 H., Leenaars, J. G. B., Ribeiro, E., Wheeler, I., Mantel, S., and Kempen, B.: SoilGrids250m: Global gridded soil  
621 information based on machine learning, *PLOS ONE*, 12, e0169748, 10.1371/journal.pone.0169748, 2017.

622 Hersbach, H., Bell, B., Berrisford, P., Hirahara, S., Horányi, A., Muñoz-Sabater, J., Nicolas, J., Peubey, C., Radu, R.,  
623 Schepers, D., Simmons, A., Soci, C., Abdalla, S., Abellan, X., Balsamo, G., Bechtold, P., Biavati, G., Bidlot, J.,  
624 Bonavita, M., De Chiara, G., Dahlgren, P., Dee, D., Diamantakis, M., Dragani, R., Flemming, J., Forbes, R., Fuentes,  
625 M., Geer, A., Haimberger, L., Healy, S., Hogan, R. J., Hólm, E., Janisková, M., Keeley, S., Laloyaux, P., Lopez, P.,  
626 Lupu, C., Radnoti, G., de Rosnay, P., Rozum, I., Vamborg, F., Villaume, S., and Thépaut, J.-N.: The ERA5 global  
627 reanalysis, *Quarterly Journal of the Royal Meteorological Society*, 146, 1999-2049, <https://doi.org/10.1002/qj.3803>,  
628 2020.

629 Herzberg, R., Pham, T. G., Kappas, M., Wyss, D., and Tran, C. T. M.: Multi-Criteria Decision Analysis for the Land  
630 Evaluation of Potential Agricultural Land Use Types in a Hilly Area of Central Vietnam, *Land*, 8, 90, 2019.

631 IFPRI: Global Spatially-Disaggregated Crop Production Statistics Data for 2020 Version 1.0, Harvard Dataverse  
632 [dataset], <https://doi.org/10.7910/DVN/SWPENT>, 2024.

633 IPCC: Climate Change 2021: The Physical Science Basis. Contribution of Working Group I to the Sixth Assessment  
634 Report of the Intergovernmental Panel on Climate Change, Cambridge University Press, 2021.

635 Ivushkin, K., Bartholomeus, H., Bregt, A. K., Pulatov, A., Kempen, B., and de Sousa, L.: Global mapping of soil salinity  
636 change, *Remote Sens Environ*, 231, 111260, <https://doi.org/10.1016/j.rse.2019.111260>, 2019.

637 Jägermeyr, J., Robock, A., Elliott, J., Müller, C., Xia, L., Khabarov, N., Folberth, C., Schmid, E., Liu, W., Zabel, F.,  
638 Rabin, S. S., Puma, M. J., Heslin, A., Franke, J., Foster, I., Asseng, S., Bardeen, C. G., Toon, O. B., and Rosenzweig,  
639 C.: A regional nuclear conflict would compromise global food security, *Proceedings of the National Academy of  
640 Sciences*, 117, 7071–7081-7071–7081, <https://doi.org/10.1073/pnas.1919049117>, 2020.

641 Jägermeyr, J., Müller, C., Ruane, A. C., Elliott, J., Balkovic, J., Castillo, O., Faye, B., Foster, I., Folberth, C., Franke, J.  
642 A., Fuchs, K., Guarin, J. R., Heinke, J., Hoogenboom, G., Iizumi, T., Jain, A. K., Kelly, D., Khabarov, N., Lange, S.,  
643 Lin, T.-S., Liu, W., Mialyk, O., Minoli, S., Moyer, E. J., Okada, M., Phillips, M., Porter, C., Rabin, S. S., Scheer, C.,  
644 Schneider, J. M., Schyns, J. F., Skalsky, R., Smerald, A., Stella, T., Stephens, H., Webber, H., Zabel, F., and  
645 Rosenzweig, C.: Climate impacts on global agriculture emerge earlier in new generation of climate and crop models,  
646 *Nature Food*, 2, 873–885-873–885, <https://doi.org/10.1038/s43016-021-00400-y>, 2021.

647 Joswig, J. S., Wirth, C., Schuman, M. C., Kattge, J., Reu, B., Wright, I. J., Sippel, S. D., Rüger, N., Richter, R.,  
648 Schaepman, M. E., van Bodegom, P. M., Cornelissen, J. H. C., Díaz, S., Hattigh, W. N., Kramer, K., Lens, F.,  
649 Niinemets, Ü., Reich, P. B., Reichstein, M., Römermann, C., Schrodt, F., Anand, M., Bahn, M., Byun, C., Campetella,  
650 G., Cerabolini, B. E. L., Craine, J. M., Gonzalez-Melo, A., Gutiérrez, A. G., He, T., Higuchi, P., Jactel, H., Kraft, N.  
651 J. B., Minden, V., Onipchenko, V., Peñuelas, J., Pillar, V. D., Sosinski, Ê., Soudzilovskaia, N. A., Weiher, E., and  
652 Mahecha, M. D.: Climatic and soil factors explain the two-dimensional spectrum of global plant trait variation, *Nature  
653 Ecology & Evolution*, 6, 36-50, 10.1038/s41559-021-01616-8, 2022.

654 Karger, D. N., Lange, S., Hari, C., Reyer, C. P. O., Conrad, O., Zimmermann, N. E., and Frieler, K.: CHELSA-W5E5:  
655 daily 1&thinsp;km meteorological forcing data for climate impact studies, *Earth Syst. Sci. Data*, 15, 2445-2464,  
656 10.5194/essd-15-2445-2023, 2023.

657 Karl, K., MacCarthy, D., Porciello, J., Chimwaza, G., Fredenberg, E., Freduah, B. S., Guarin, J., Mendez Leal, E.,  
658 Kozłowski, N., Narh, S., Sheikh, H., Valdivia, R., Wesley, G., Van Deynze, A., van Zonneveld, M., and Yang, M.:  
659 Opportunity Crop Profiles for the Vision for Adapted Crops and Soils (VACS) in Africa,  
660 <https://doi.org/10.7916/7msa-yy32>, 2024.

661 Knüttel, M. and Zabel, F.: CropSuite User Manual, <https://doi.org/10.5281/zenodo.14196315>, 2024.

662 Lang, A. and Poschlod, B.: Updating catastrophe models to today's climate – An application of a large ensemble approach  
663 to extreme rainfall, *Climate Risk Management*, 44, 100594, <https://doi.org/10.1016/j.crm.2024.100594>, 2024.

664 Lemma, E., Upadhyaya, S., and Ramsankaran, R.: Investigating the performance of satellite and reanalysis rainfall  
665 products at monthly timescales across different rainfall regimes of Ethiopia, *International Journal of Remote Sensing*,  
666 40, 4019-4042, 10.1080/01431161.2018.1558373, 2019.

667 Li, S., Tompkins, A. M., Lin, E., and Ju, H.: Simulating the impact of flooding on wheat yield – Case study in East China,  
668 *Agr Forest Meteorol*, 216, 221-231, <https://doi.org/10.1016/j.agrformet.2015.10.014>, 2016.

669 Maleki, F., Kazemi, H., Siahmarguee, A., and Kamkar, B.: Development of a land use suitability model for saffron  
670 (*Crocus sativus* L.) cultivation by multi-criteria evaluation and spatial analysis, *Ecol Eng*, 106, 140-153,  
671 <https://doi.org/10.1016/j.ecoleng.2017.05.050>, 2017.

672 Marke, T., Mauser, W., Pfeiffer, A., Zängl, G., Jacob, D., and Strasser, U.: Application of a hydrometeorological model  
673 chain to investigate the effect of global boundaries and downscaling on simulated river discharge, *Environ Earth Sci*,  
674 71, 4849-4868, 10.1007/s12665-013-2876-z, 2014.

675 Meier, J., Zabel, F., and Mauser, W.: A global approach to estimate irrigated areas – a comparison between different data  
676 and statistics, *Hydrology and Earth System Sciences*, 22, 1119–1133-1119–1133, 2018.

677 Molina Bacca, E. J., Stevanović, M., Bodirsky, B. L., Karstens, K., Chen, D. M.-C., Leip, D., Müller, C., Minoli, S.,  
678 Heinke, J., Jägermeyr, J., Folberth, C., Iizumi, T., Jain, A. K., Liu, W., Okada, M., Smerald, A., Zabel, F., Lotze-  
679 Campen, H., and Popp, A.: Uncertainty in land-use adaptation persists despite crop model projections showing lower  
680 impacts under high warming, *Communications Earth & Environment*, 4, 284, 10.1038/s43247-023-00941-z, 2023.



681 Monteleone, B., Giusti, R., Magnini, A., Arosio, M., Domeneghetti, A., Borzì, I., Petruccelli, N., Castellarin, A.,  
682 Bonaccorso, B., and Martina, M. L. V.: Estimations of Crop Losses Due to Flood Using Multiple Sources of  
683 Information and Models: The Case Study of the Panaro River, *Water*, 15, 1980, 2023.

684 Müller, C., Ouédraogo, W. A., Schwarz, M., Barteit, S., and Sauerborn, R.: The effects of climate change-induced  
685 flooding on harvest failure in Burkina Faso: case study, *Frontiers in Public Health*, 11, 10.3389/fpubh.2023.1166913,  
686 2023.

687 Müller, C., Jägermeyr, J., Franke, J. A., Ruane, A. C., Balkovic, J., Ciais, P., Dury, M., Falloon, P., Folberth, C., Hank,  
688 T., Hoffmann, M., Izaurrealde, R. C., Jacquemin, I., Khabarov, N., Liu, W., Olin, S., Pugh, T. A. M., Wang, X.,  
689 Williams, K., Zabel, F., and Elliott, J. W.: Substantial Differences in Crop Yield Sensitivities Between Models Call  
690 for Functionality-Based Model Evaluation, *Earth's Future*, 12, e2023EF003773,  
691 <https://doi.org/10.1029/2023EF003773>, 2024.

692 Muthoni, F. K., Odongo, V. O., Ochieng, J., Mugalavai, E. M., Mourice, S. K., Hoesche-Zeledon, I., Mwila, M., and  
693 Bekunda, M.: Long-term spatial-temporal trends and variability of rainfall over Eastern and Southern Africa,  
694 *Theoretical and Applied Climatology*, 137, 1869-1882, 10.1007/s00704-018-2712-1, 2019.

695 Orlov, A., Jägermeyr, J., Müller, C., Daloz, A. S., Zabel, F., Minoli, S., Liu, W., Lin, T.-S., Jain, A. K., Folberth, C.,  
696 Okada, M., Poschlod, B., Smerald, A., Schneider, J. M., and Sillmann, J.: Human heat stress could offset potential  
697 economic benefits of CO2 fertilization in crop production under a high-emissions scenario, *One Earth*, 7, 1250-1265,  
698 <https://doi.org/10.1016/j.oneear.2024.06.012>, 2024.

699 Pasley, H. R., Huber, I., Castellano, M. J., and Archontoulis, S. V.: Modeling Flood-Induced Stress in Soybeans, *Frontiers*  
700 *in Plant Science*, 11, 10.3389/fpls.2020.00062, 2020.

701 Pelletier, J. D., Broxton, P. D., Hazenberg, P., Zeng, X., Troch, P. A., Niu, G.-Y., Williams, Z., Brunke, M. A., and  
702 Gochis, D.: A gridded global data set of soil, intact regolith, and sedimentary deposit thicknesses for regional and  
703 global land surface modeling, *Journal of Advances in Modeling Earth Systems*, 8, 41-65,  
704 <https://doi.org/10.1002/2015MS000526>, 2016.

705 Peter, B. G., Messina, J. P., Lin, Z., and Snapp, S. S.: Crop climate suitability mapping on the cloud: a geovisualization  
706 application for sustainable agriculture, *Scientific Reports*, 10, 15487, 10.1038/s41598-020-72384-x, 2020.

707 Ramirez-Villegas, J., Jarvis, A., and Läderach, P.: Empirical approaches for assessing impacts of climate change on  
708 agriculture: The EcoCrop model and a case study with grain sorghum, *Agr Forest Meteorol*, 170, 67-78,  
709 <https://doi.org/10.1016/j.agrformet.2011.09.005>, 2013.

710 Ranjitkar, S., Sujakhu, N. M., Merz, J., Kindt, R., Xu, J., Matin, M. A., Ali, M., and Zomer, R. J.: Suitability Analysis  
711 and Projected Climate Change Impact on Banana and Coffee Production Zones in Nepal, *PLOS ONE*, 11, e0163916,  
712 10.1371/journal.pone.0163916, 2016.

713 Ruane, A. C., Rosenzweig, C., Asseng, S., Boote, K. J., Elliott, J., Ewert, F., Jones, J. W., Martre, P., McDermid, S. P.,  
714 Müller, C., Snyder, A., and Thorburn, P. J.: An AgMIP framework for improved agricultural representation in  
715 integrated assessment models, *Environmental Research Letters*, 12, 125003, 10.1088/1748-9326/aa8da6, 2017.

716 Schneider, J. M., Zabel, F., and Mauser, W.: Global inventory of suitable, cultivable and available cropland under  
717 different scenarios and policies, *Scientific Data*, 9, <https://doi.org/10.1038/s41597-022-01632-8>, 2022a.

718 Schneider, J. M., Zabel, F., and Mauser, W.: Global inventory of suitable, cultivable and available cropland under  
719 different scenarios and policies, *Scientific Data*, 9, 527, 10.1038/s41597-022-01632-8, 2022b.

720 Schneider, J. M., Delzeit, R., Neumann, C., Heimann, T., Seppelt, R., Schuenemann, F., Söder, M., Mauser, W., and  
721 Zabel, F.: Effects of profit-driven cropland expansion and conservation policies, *Nature Sustainability*, 7, 1335-1347,  
722 10.1038/s41893-024-01410-x, 2024.

723 Steinkopf, J. and Engelbrecht, F.: Verification of ERA5 and ERA-Interim precipitation over Africa at intra-annual and  
724 interannual timescales, *Atmospheric Research*, 280, 106427, <https://doi.org/10.1016/j.atmosres.2022.106427>, 2022.

725 Sun, Y., Solomon, S., Dai, A., and Portmann, R. W.: How Often Does It Rain?, *Journal of Climate*, 19, 916-934,  
726 10.1175/jcli3672.1, 2006.

727 Sys, C. O., van Ranst, E., and Debaveye, J.: Land evaluation: Part II Methods in Land Evaluation, G.A.D.C, Brussels,  
728 1991.

729 Sys, C. O., van Ranst, E., Debaveye, J., and Beernaert, F.: Land evaluation: Part III Crop requirements, G.A.D.C,  
730 Brussels, 1993.

731 Tebaldi, C., Dorheim, K., Wehner, M., and Leung, R.: Extreme metrics from large ensembles: investigating the effects  
732 of ensemble size on their estimates, *Earth Syst. Dynam.*, 12, 1427-1501, 10.5194/esd-12-1427-2021, 2021.

733 Terblanche, D., Lynch, A., Chen, Z., and Sinclair, S.: ERA5-Derived Precipitation: Insights from Historical Rainfall  
734 Networks in Southern Africa, *Journal of Applied Meteorology and Climatology*, 61, 1473-1484,  
735 <https://doi.org/10.1175/JAMC-D-21-0096.1>, 2022.

736 van Zonneveld, M., Kindt, R., McMullin, S., Achigan-Dako, E. G., N'Danikou, S., Hsieh, W.-h., Lin, Y.-r., and Dawson,  
737 I. K.: Forgotten food crops in sub-Saharan Africa for healthy diets in a changing climate, *Proceedings of the National  
738 Academy of Sciences*, 120, e2205794120, 10.1073/pnas.2205794120, 2023.

739 Verdin, A., Funk, C., Peterson, P., Landsfeld, M., Tuholske, C., and Grace, K.: Development and validation of the  
740 CHIRTS-daily quasi-global high-resolution daily temperature data set, *Scientific Data*, 7, 303, 10.1038/s41597-020-  
741 00643-7, 2020.

742 Vogel, E., Donat, M. G., Alexander, L. V., Meinshausen, M., Ray, D. K., Karoly, D., Meinshausen, N., and Frieler, K.:  
743 The effects of climate extremes on global agricultural yields, *Environmental Research Letters*, 14, 054010,  
744 10.1088/1748-9326/ab154b, 2019.

745 Wang, F., Tian, D., Lowe, L., Kalin, L., and Lehrter, J.: Deep Learning for Daily Precipitation and Temperature  
746 Downscaling, *Water Resources Research*, 57, e2020WR029308, <https://doi.org/10.1029/2020WR029308>, 2021.

747 Yu, Q., You, L., Wood-Sichra, U., Ru, Y., Joglekar, A. K. B., Fritz, S., Xiong, W., Lu, M., Wu, W., and Yang, P.: A  
748 cultivated planet in 2100 – Part 2: The global gridded agricultural-production maps, *Earth Syst. Sci. Data*, 12, 3545-  
749 3572, 10.5194/essd-12-3545-2020, 2020.

750 Zabel, F.: Global Agricultural Land Resources – A High Resolution Suitability Evaluation and Its Perspectives until 2100  
751 under Climate Change Conditions (v3.0) Zenodo [dataset], <https://doi.org/10.5281/zenodo.5982577>, 2022.

752 Zabel, F. and Knüttel, M.: CropSuite Version 1.0 User Manual, 21.05.2024.

753 Zabel, F., Putzenlechner, B., and Mauser, W.: Global Agricultural Land Resources – A High Resolution Suitability  
754 Evaluation and Its Perspectives until 2100 under Climate Change Conditions, *PLoS ONE*, 9, e107522-e107522,  
755 <https://doi.org/10.1371/journal.pone.0107522>, 2014.

756